Electronic Supplementary Material (ESI) for Soft Matter.
This journal is © The Royal Society of Chemistry 2018

Electronic Supplementary Information

Multi-stimuli-responsive supramolecular gel constructed by pillar[5]arene-based pseudorotaxanes for efficient detection and separation of multi-analytes in water solution

You-Ming Zhang* Yong-Fu Li, Hu Fang, Jun-Xia He, Bi-Rong Yong, Hong Yao, Tai-Bao Wei and Qi Lin*

Key Laboratory of Eco-Environment-Related Polymer Materials, Ministry of Education of China, Key Laboratory of Polymer Materials of Gansu Province, College of Chemistry and Chemical Engineering, Northwest Normal University, Lanzhou, Gansu, 730070, P. R. China.

Table of Contents

Table S2. Optimum water content of gelation conditions.

Fig. S19 Fluorescence spectra of supramolecular gel **WP5-PN-G** (in gelated state, 10.5 %, w/v) and solution in the DMSO-H_2O (1:1, v/v) system (λ_{ex} =365 nm).

Fig. S20 Fluorescence spectra of **WP5** (c = 90 mM), **PN** (c = 87 mM), **WP5-PN** sol (c = 90 mM, T = 85 °C > T_{gel}) and the **WP5-PN-G** (in the DMSO-H_2O (1:1, v/v) system, c = 90 mM, T = 20 °C < T_{gel}, λ_{ex} =365 nm).

Fig. S21 Partial ^{1}H NMR spectra of **WP5** (0.017 mol/L) in DMSO-d_6 with increasing amounts of **PN**, (a) Free **WP5**; (b) 0.5 equiv. (c) 2.0 equiv. (d) Free **PN**.

Fig. S22 2D NOESY NMR spectrum (600 MHz, 298 K) of 50.0 mM **WP5** and **PN** in DMSO-d_6 solution.

Fig. S23 ESI-MS spectrum of the host-guest complex formed between **WP5** and **PN**.

Fig. S24 ^{1}H NMR spectra (600 MHz, 298 K) of **WP5-PN** in DMSO-d_6 at various concentrations: (a) 1.0 mM; (b) 2.0 mM; (c) 5.0 mM; (d) 10.0 mM; (e) 20.0 mM.

Fig. S25 XRD diagrams of xerogel of **WP5-PN-G**, metallogel of **WP5-PN-FeG**, xerogel of **WP5-PN-FeG +F$^-$**.

Fig. S26 XRD diagrams of xerogel of **WP5-PN-G**, metallogel of **WP5-PN-CuG** and xerogel of **WP5-PN-CuG +CN$^-$**.

Fig. S27 Partial ^{1}H NMR spectra (600 MHz, DMSO-d_6, 298 K) of **WP5-**

PN and CH_3COOH at various concentrations: (a) 5.0 mM; (b) 8.0 mM; (c) 10.0 mM; (d) 15.0 mM; (e) 20.0 mM.

Fig. S28 Photographs of organogel of **WP5-PN-G** (10.5% w/v) in DMSO-H_2O (1:1, v/v) system and organogels of **WP5-PN-G** in the presence of various metal ions (Zn^{2+}, Pb^{2+}, Cd^{2+}, Al^{3+}, Cr^{3+}, Ni^{2+}, Co^{2+}, Cu^{2+}, Hg^{2+}, Fe^{3+}, Ba^{2+}, Ag^{+}, Mg^{2+}, Ca^{2+}, Tb^{3+}, La^{3+} and Eu^{3+}) under UV light.

Fig. S29 Fluorescence spectra of supramolecular gel (a) **WP5-PN-G** and **WP5-PN-FeG** (10.5%, in DMSO-H_2O (v:v = 1:1) binary solution, **WP5-PN** = 1:1). (b) The fluorescence spectra of **WP5-PN-G** (10.5%, in DMSO-H_2O (v:v = 1:1) binary solution, **WP5-PN** = 1:1) with increasing concentration of Fe^{3+} (using 0.1 mol L^{-1} Fe^{3+} water solution as the Fe^{3+} sources), λ_{ex} = 365 nm.

Fig. S30 Plot of the intensity at 492 nm for a mixture of **WP5-PN-G** and Fe^{3+} (λ_{ex}= 365 nm).

Fig. S31 Plot of the intensity at 492 nm for a mixture of **WP5-PN-G** and Cu^{2+} in DMSO-H_2O (1:1, v/v) solution (λ_{ex}= 365 nm).

Table S3. A part of the literatures about the LOD (mol/L) of cations and anions (Fe^{3+}, Cu^{2+}, F^- and CN^-) were provided in the followed table.

Table S4 Adsorption percentage of **WP5-PN-G** for Fe^{3+} and Cu^{2+}.

Fig. S32 (a) Photographs of **WP5–PN-CuG** in the DMSO-H_2O (1:1, v/v) system (10.5 %, w/v) and **WP5–PN-CuG** in the presence of various

anions under UV light. (b) Fluorescence spectra of **WP5–PN-CuG** and **WP5–PN-CuG** (in gelated state) in the presence of various anions, (λ_{ex} =365 nm).

Fig. S33 Fluorescence spectra of supramolecular metallogel **WP5-PN-CuG** (10.5%, w/v) in DMSO-H_2O (1:1, v/v) solution with increasing concentration of CN^- (using 1.0 M NaCN water solution as the CN^- source), λ_{ex} = 365 nm.

Fig. **S34** FT-IR spectra of xerogel of **WP5-PN-G**, metallogel **WP5-PN-FeG** and **WP5-PN-FeG +F$^-$**.

Fig. S35 FT-IR spectra of xerogel of **WP5-PN-G**, metallogel **WP5-PN-CuG** and **WP5-PN-CuG +CN$^-$**.

Fig. S36 ESI-MS spectrum of **WP5-PN**-Fe^{3+}.

Fig. S37 ESI-MS spectrum of **WP5-PN**-Cu^{2+}.

Fig. S38 Absorbance spectra of **WP5-PN-G** (2.0×10^{-5} M) in DMSO-H_2O (1:1, v/v) solution upon the addition of Fe^{3+} (5.0 equiv.) and F^- (20.0 equiv.). Inset: photograph showing the change in color of the solution of **WP5-PN-G** in DMSO-H_2O (1:1, v/v) solution after addition of Fe^{3+} and F^- at room temperature.

Fig. S39 Partial ^1H NMR spectra (600 MHz, DMSO-d_6, 298 K) of (a) **WP5-PN** in the presence of varying amounts of Cu^{2+} and (b) **WP5-PN** + Cu^{2+} in the presence of varying amounts of CN^-.

Fig. S40 Emission spectra showing the reversible evidence between

WP5-PN-G and Fe^{3+} by introduction of F^- (λ_{ex} = 365 nm).

Fig. S41 Fluorescent ‘‘Off–On–Off’’ cycles of **WP5-PN-G** controlled by the alternating addition of Cu^{2+} and CN^- (λ_{ex} = 365 nm).

Fig. S42 (a) Recyclable separation of Fe^{3+} (λ_{ex} = 365 nm), (b) Recyclable separation of Cu^{2+} (λ_{ex} = 365 nm).

Materials and physical methods

All anions were used as tetrabutylammonium salts, which were purchased from Alfa Aesar and used as received. All metal ions were prepared from the perchlorate salts. Other reagents used in the study were of analytical grade. Fresh double distilled water was used throughout the experiment. All other reagents and solvents were commercially available at analytical grade and were used without further purification. ^{1}H NMR spectra were recorded on Mercury-400BB spectrometer (400MHz) and Bruker Digital RF spectrometer (300MHz). ^{1}H chemical shifts are reported in ppm downfield from tetramethylsilane (TMS, TM scale with the solvent resonances as internal standards). Mass spectra were performed on a Bruker Esquire 3000 plus mass spectrometer (Bruker-FranzenAnalytik GmbH Bremen, Germany) equipped with ESI interface and ion trap analyzer. The X-ray diffraction analysis (XRD) was performed on a Rigaku D/Max-2400 X-Ray Diffractometer. The morphologies and sizes of the xerogels were characterized using field emission scanning electron microscopy (FE-SEM, JSM-6701F) at an accelerating voltage of 8 kV. The infrared spectra were performed on a Digilab FTS-3000 Fourier transform-infrared spectrophotometer.Melting points were measured on an X-4 digital melting-point apparatus (uncorrected). Ultraviolet-visible (UV-vis) spectra were recorded on a Shimadzu UV-2550 spectrometer. Fluorescence spectra were recorded on a Shimadzu RF-5301PC spectrofluorophotometer.

2. Synthesis and characterizations of compound PN and **WP5**.

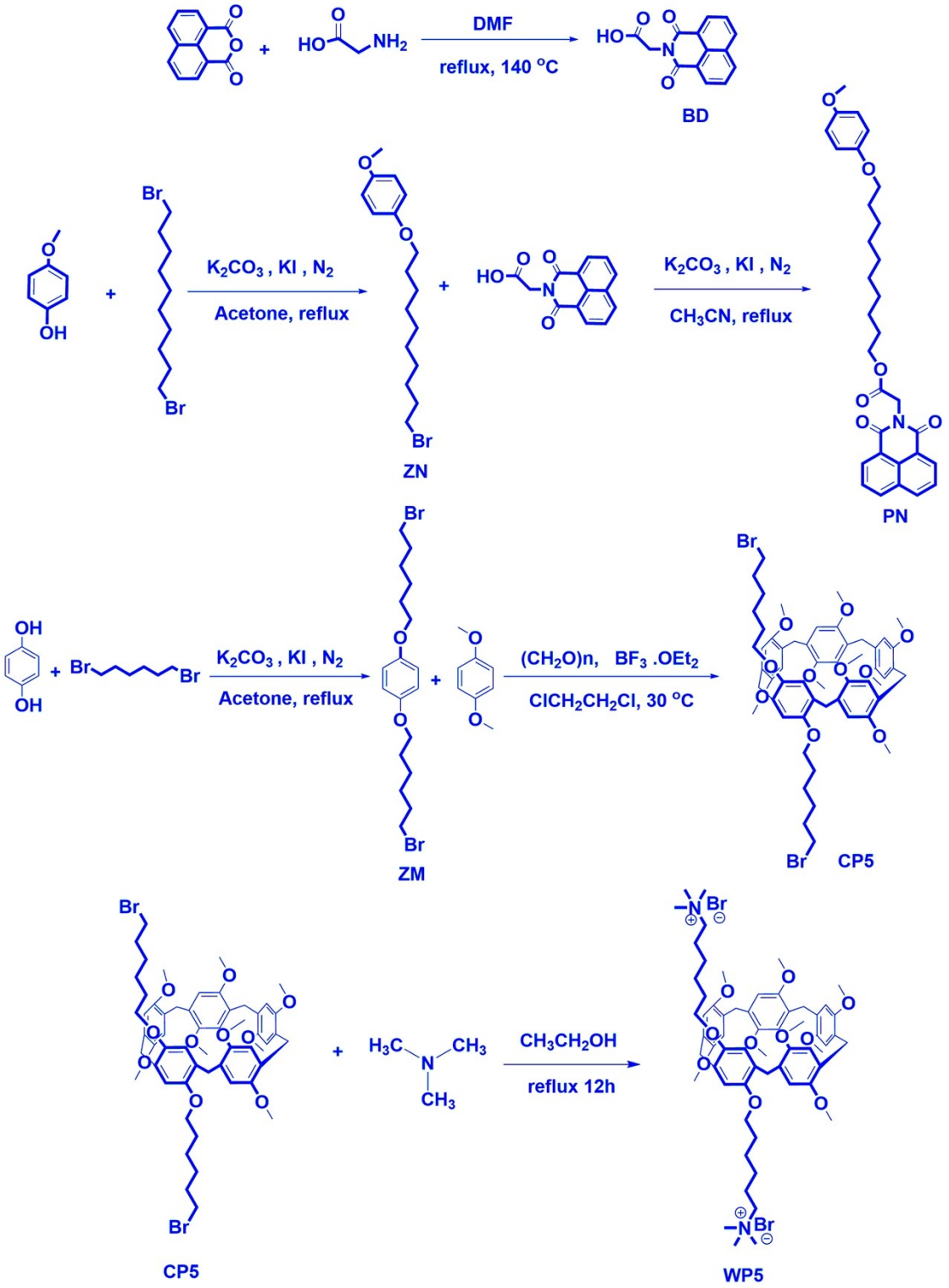

Scheme S1 Synthesis of compound **PN** and **WP5**.

Synthesis of compound BD: A mixture of 1,8-naphthalenedicarboxylic anhydride (1.98 g, 10.0 mmol), glycine (1.13 g, 15.0 mmol) in anhydrous

DMF (20 mL) was stirred at 140 °C reflux for 24 h. After cooling to room temperature, add water and the precipitate was filtered, then with acetonitrile recrystallization get gray powder product BD. yield 65%; m.p. >300 °C; ^{1}H NMR (600 MHz, DMSO-d_6) δ 13.06 (s, 1H),8.48 (m, 4H), 7.88 (t, 2H), 4.72 (s, 2H). ESI-MS m/z: [2(**BD**)+Na]$^+$ Calcd for $C_{28}H_{18}N_2NaO_8$, 533.0961; Found 533.09.

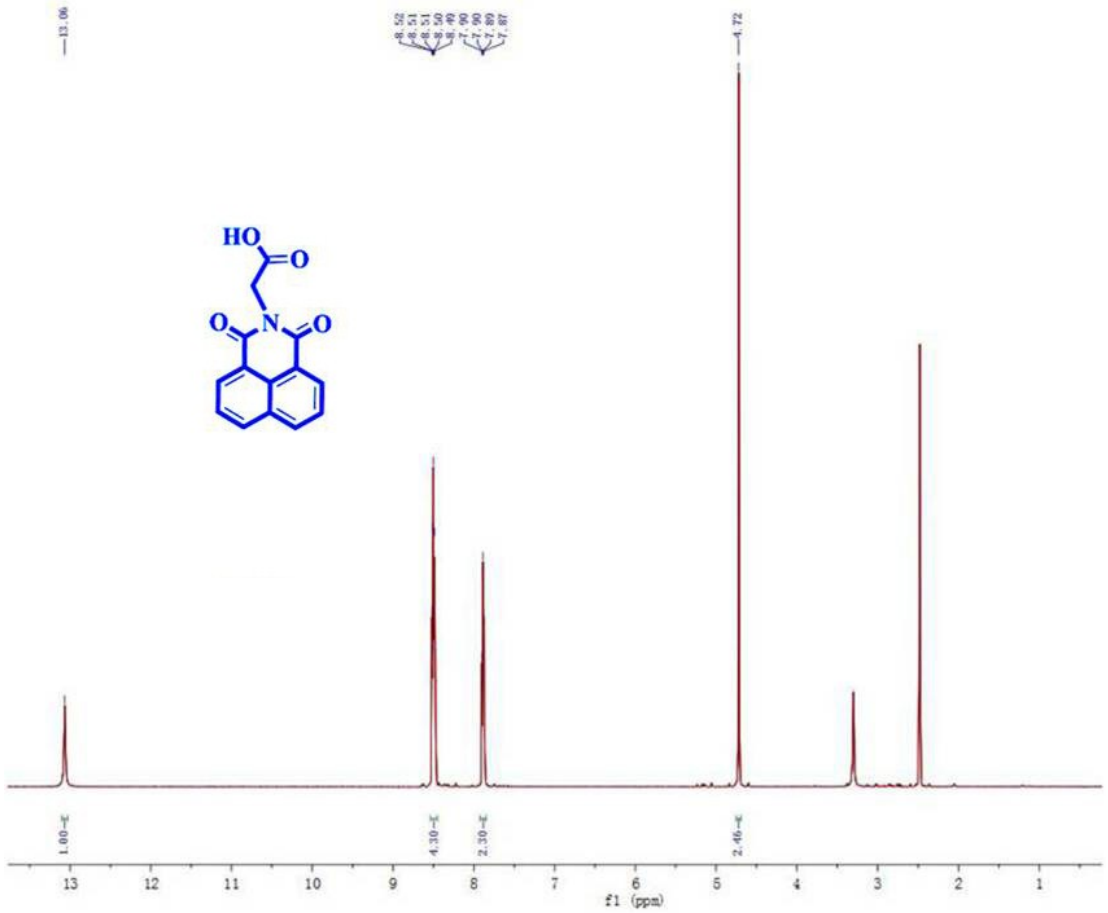

Fig. S1 ^{1}H NMR spectrum of **BD** in DMSO-d_6.

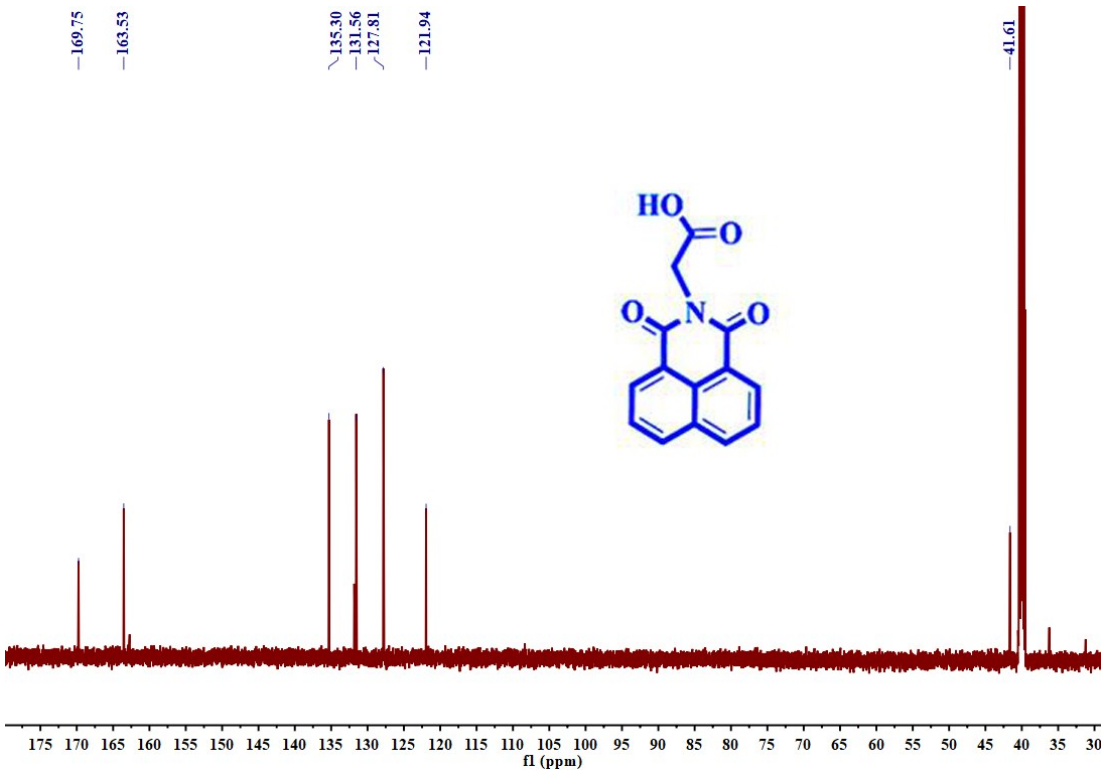

Fig. S2 ^{13}C NMR spectra (151MHz, DMSO-d_6) of **ND**.

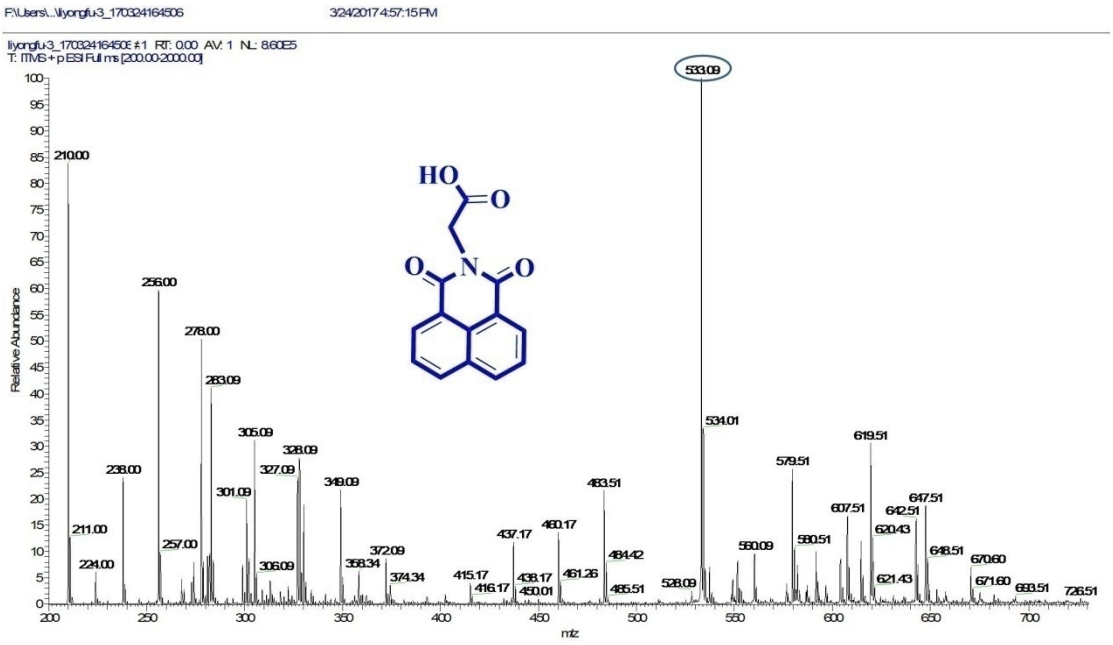

Fig. S3 ESI-MS spectrum of **BD**.

Synthesis of compound PN: A mixture of 4-methoxyphenol (2.48 g, 20.0 mmol), K_2CO_3 (13.82 g, 100 mmol), KI (3.32 g, 20 mmol), 1,10-dibormodecane (24.01 g, 80 mmol) and acetone (400.0 mL) were added

to a 500 mL round-bottom flask under nitrogen atmosphere. The reaction mixture was stirred at 65 °C for 72 h. After the solid was filtered off, the solvent was evaporated and the residue was dissolve in CH_2Cl_2. The crude product was purified by silica gel column chromatography using petroleum ether/ethyl acetate (V/V = 50:1) as the eluent, compound **ZN** as white solid (6.53 g, yield 95%) was obtained. Mp: 60-64 °C. ^{1}H NMR (600 MHz, $CDCl_3$) δ 6.83 (s, 4H), 3.90 (t, *J* = 6.6 Hz, 2H), 3.76 (s, 3H), 3.40 (t, *J* = 6.9 Hz, 2H), 1.84 (dp, *J* = 12.9, 7.2 Hz, 2H), 1.75 (p, *J* = 6.8 Hz, 2H), 1.45 – 1.42 (m, 2H), 1.39 – 1.17 (m, 10H). ^{13}C NMR ($CDCl_3$, 151 MHz), δ/ppm: 153.64, 153.27, 115.41, 114.59, 68.62, 55.73, 34.01, 32.81, 29.42, 29.36, 29.33, 29.32, 28.72, 28.14, 26.02. ESI-MS m/z: calcd for $C_{17}H_{27}BrO_2$ [**ZN**]: 342.12; found: 342.01.

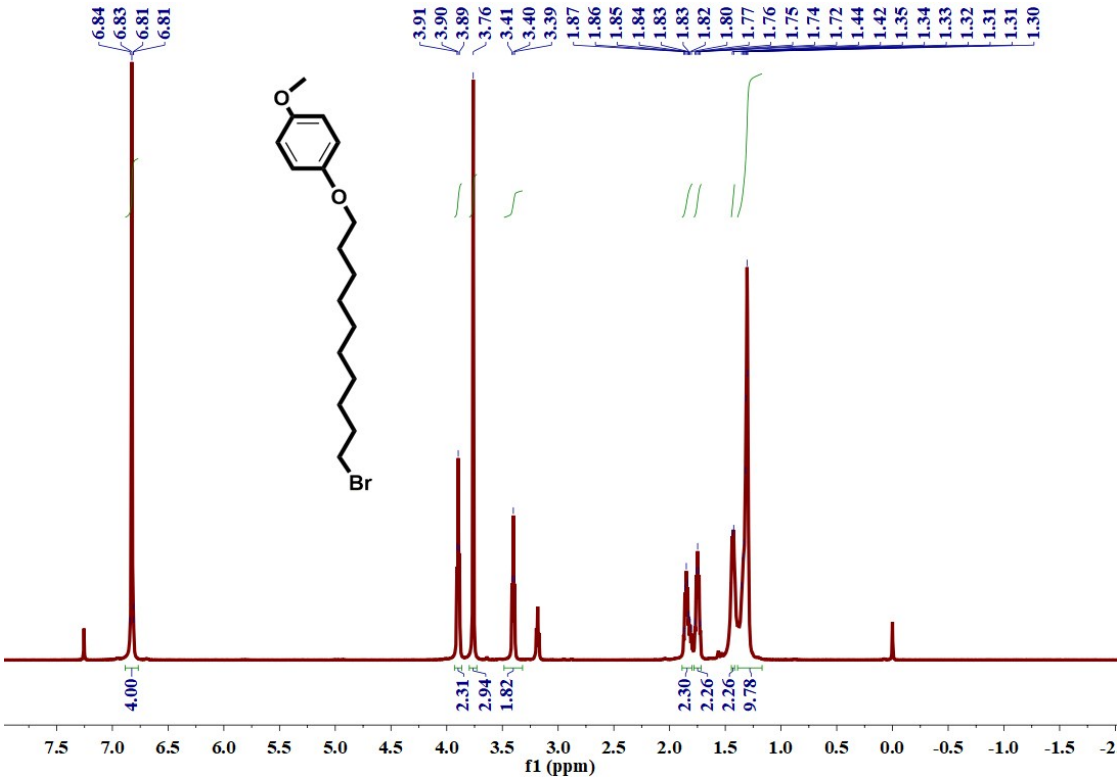

Fig. S4 ^{1}H NMR spectrum of compound **ZN** in $CDCl_3$.

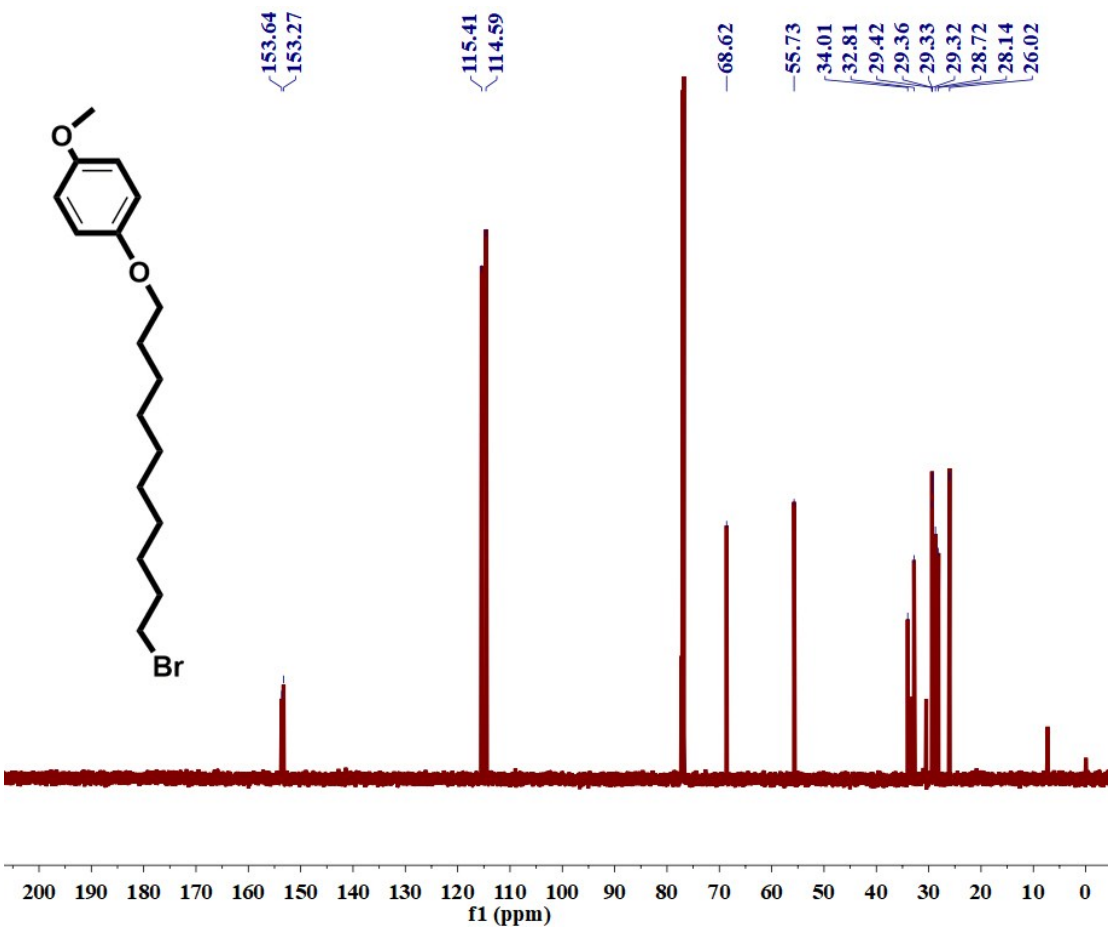

Fig. S5 ^{13}C NMR spectrum of compound **ZN** in $CDCl_3$.

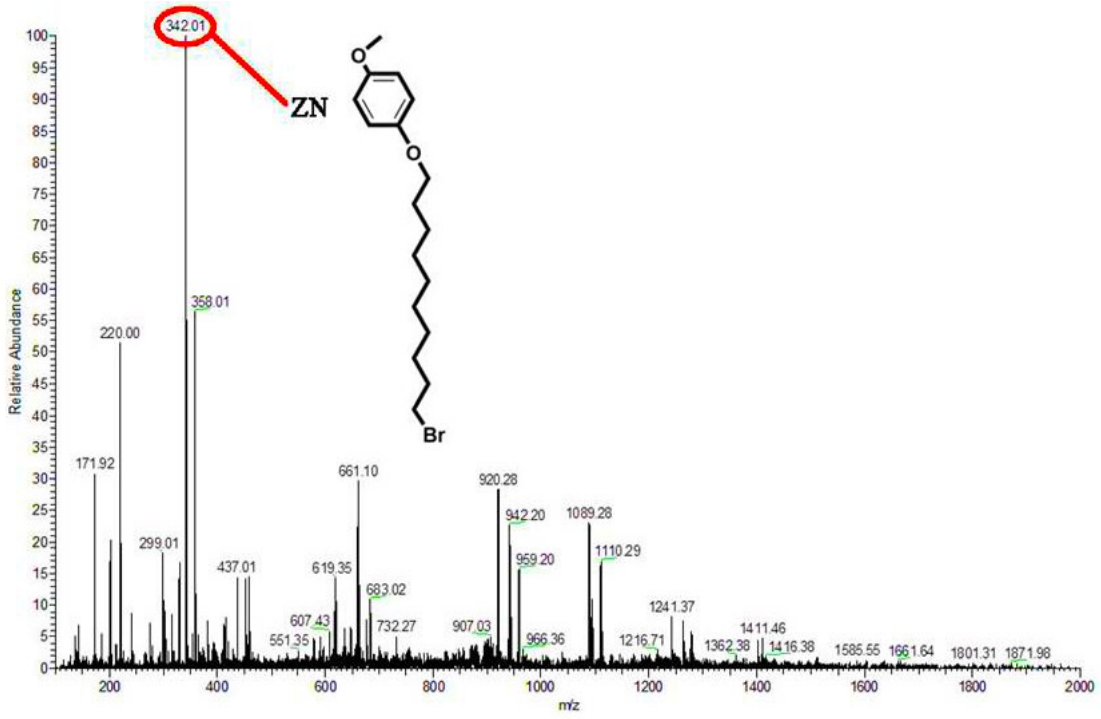

Fig. S6 ESI-MS spectrum of compound **ZN**.

In a 100 mL round bottom flask, compound **ZN** (0.43 g, 1.25 mmol), K_2CO_3 (1.55 g, 11.25 mmol), KI (0.08 g, 0.5 mmol), **BD** (0.26 g, 1.0 mmol) and acetonitrile (75 ml) was added and the reaction mixture was stirred for 48 h at 85 ^oC . After removal of the inorganic salt by filtration, the solvent was evaporated and afford the crude product, which was isolated by flash column chromatography using petroleum ether/ethyl acetate (10:1). The fractions containing the product were combined and concentrated under vacuum to give **PN** (0.45 g, yield 85%) as a white solid. Mp: 90 - 91 ^oC. ^1H NMR (600 MHz, DMSO-d_6) δ 8.51 (dd, J = 12.7, 7.8 Hz, 4H), 7.91 – 7.86 (m, 2H), 6.81 (d, J = 1.4 Hz, 4H), 4.80 (s, 2H), 4.07 (t, J = 6.4 Hz, 2H), 3.84 (t, J = 6.5 Hz, 2H), 3.65 (d, J = 3.6 Hz, 3H), 1.65 – 1.59 (m, 2H), 1.54 – 1.49 (m, 2H), 1.35 – 1.29 (m, 2H), 1.23 – 1.10 (m, 10H). ^{13}C NMR (101 MHz, DMSO-d_6) δ 168.55 , 163.74 , 154.01 , 153.47 , 135.54 , 131.79 , 127.98 , 122.14 , 116.10 , 115.34 , 68.71 , 65.60 , 56.10 , 41.91 , 29.41 , 29.12 , 25.88 . ESI-MS m/z: $[PN+Na]^+$ Calcd for $C_{31}H_{35}NNaO_6$, 540.24; Found 540.26.

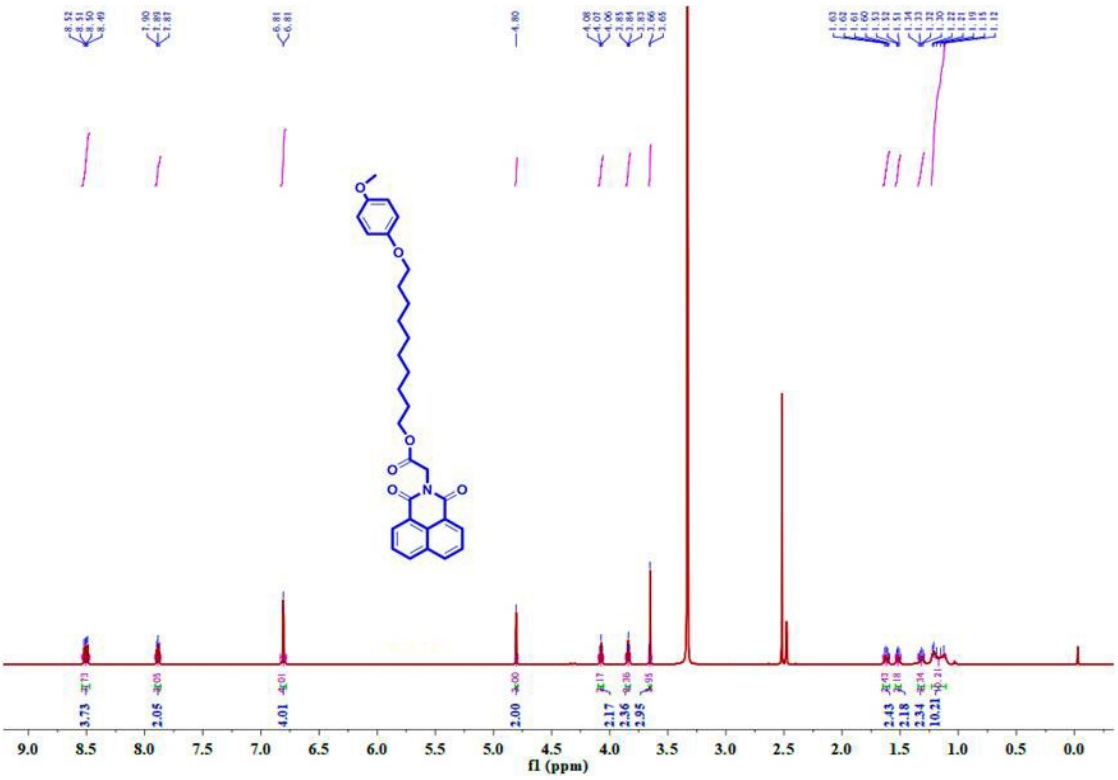

Fig. S7 ^{1}H NMR spectra (600 MHz, DMSO-d_6) of **PN**.

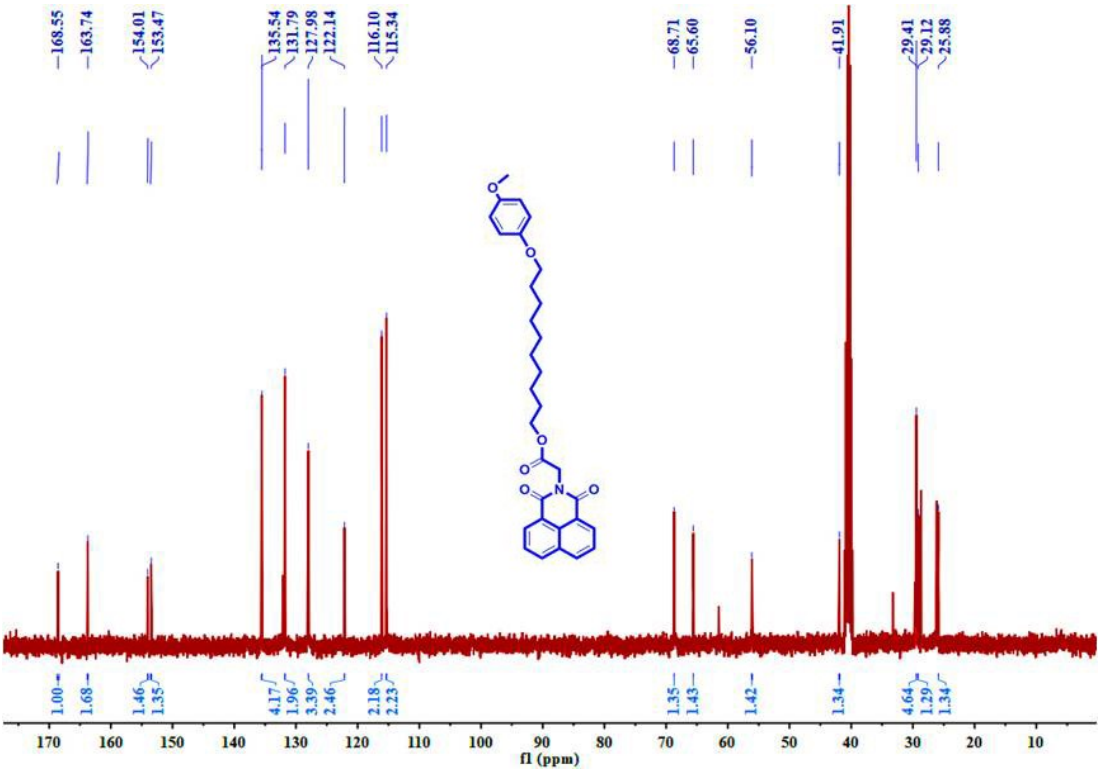

Fig. S8 ^{13}C NMR spectra (151 MHz, DMSO-d_6) of **PN**.

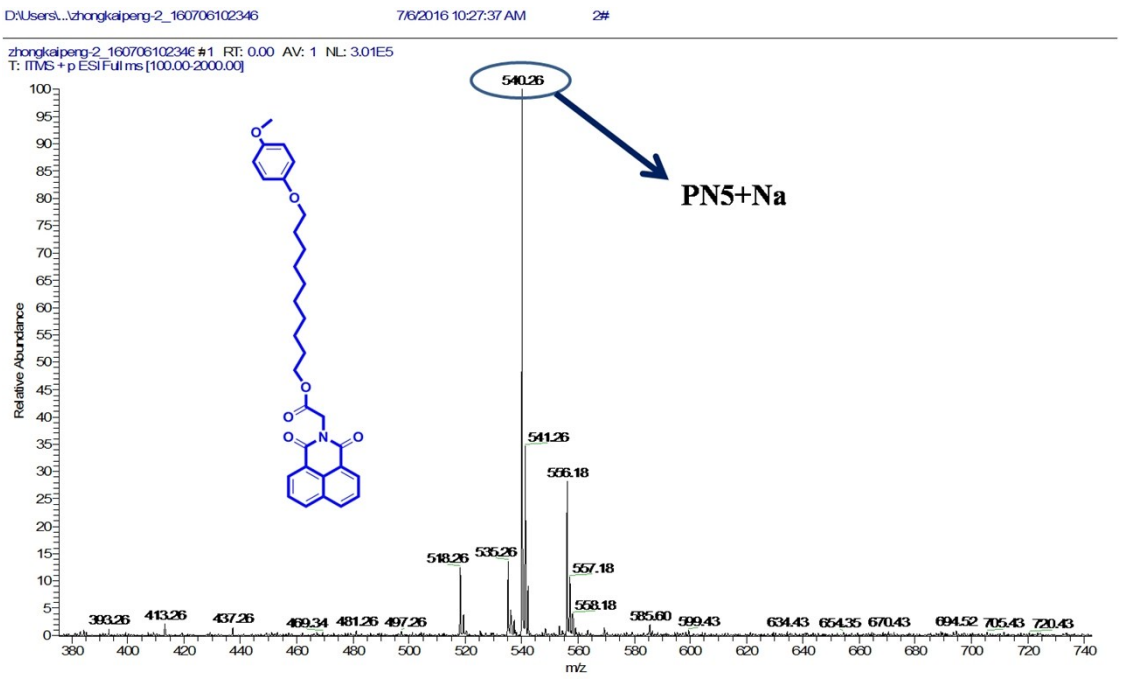

Fig. S9 ESI-MS spectrum of **PN**.

Synthesis of 1, 4-bis(4-bromohexyloxy)benzene ZM: Hydroquinone (2.3 g, 20.0 mmol), K_2CO_3 (16.6 g, 120 mmol), KI (6.6 g, 40 mmol), 1, 4-dibromobutane (34.6 g, 160 mmol) and acetone (400.0 mL) were added in a 500mL round bottom flask stirred at room temperature. The reaction mixture was stirred at reflux for 1.5 days. After the solid was filtered off, the solvent was evaporated and the residue was dissolved in CH_2Cl_2. Column chromatography (silica gel; petroleum ether: CH_2Cl_2 = 10:1) afforded a white solid (6.0 g yield 70%). m.p.: 87 ^oC. ^1H NMR (600 MHz, $CDCl_3$) δ 6.81 (s, 4H), 3.90 (t, 4H), 3.42 (t, 4H), 1.89 (m, 4H), 1.77 (m, 4H), 1.49 (m, 8H). ESI-MS m/z: $[ZM+H]^+$ Calcd for $C_{18}H_{29}Br_2O_2$, 437.05; Found 437.01.

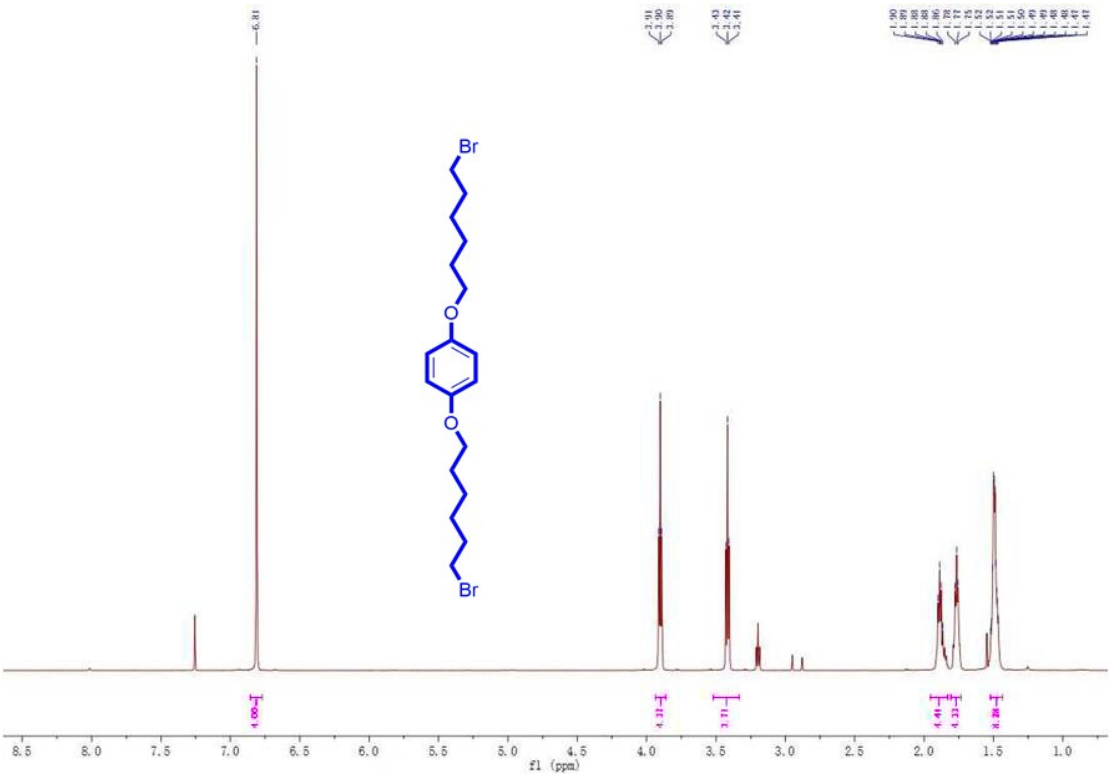

Fig. S10 ^{1}H NMR spectra (600 MHz, $CDCl_3$) of **ZM**.

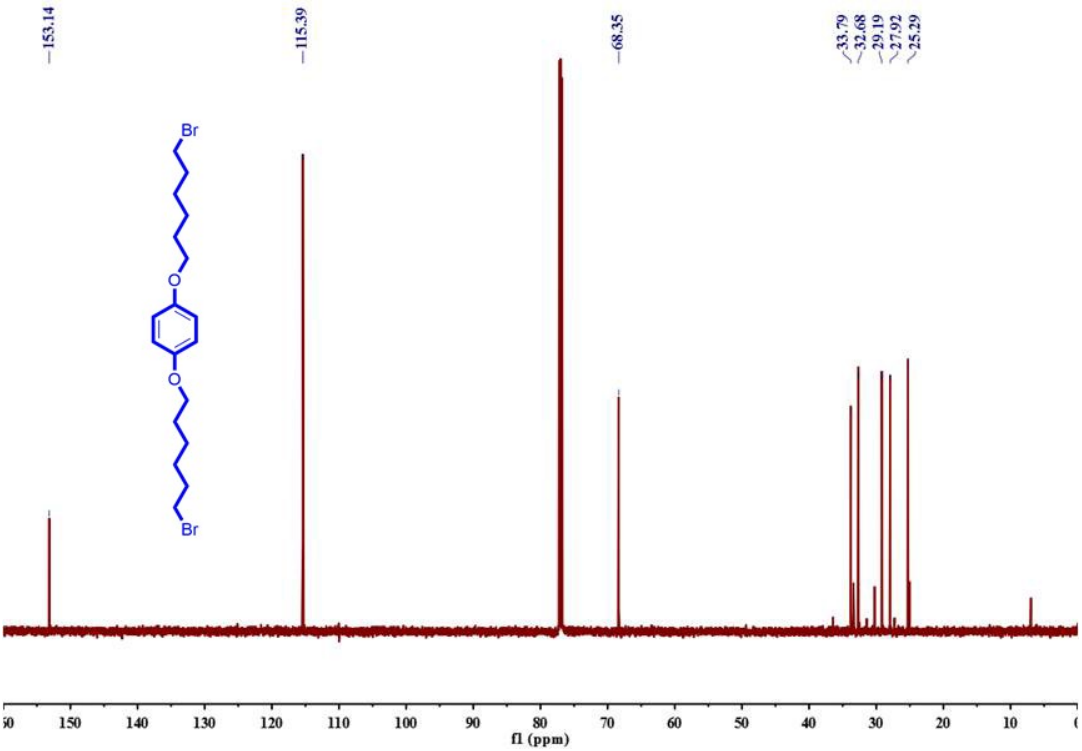

Fig. S11 ^{13}C NMR spectra (151 MHz, $CDCl_3$) of **ZM**.

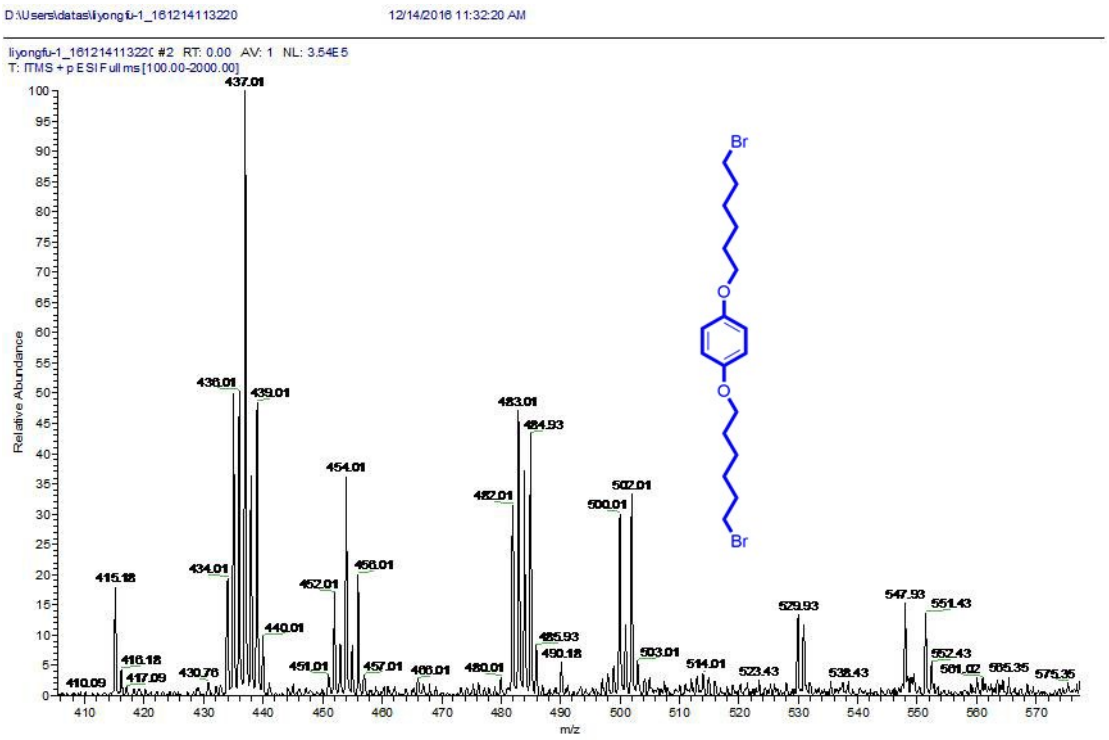

Fig. S12 ESI-MS spectrum of **ZM**.

Synthesis of Copillar[5]arene CP5. To a solution of 1, 4-bis (4-bromohexyoxy) benzene (1.9 g, 5.0 mmol) and 1,4-dimethoxybenzene (2.76 g, 20.0 mmol) in 1, 2-dichloroethane (200 mL), paraformaldehyde (0.75 g, 25.0 mmol) was added under nitrogen atmosphere. Then boron trifluoride diethyl etherate (6.75 mL, 25 mmol) was added to the solution and the mixture was stirred at room temperature for 4 h and concentrated by rotary evaporation. The resultant oil was dissolved in CH_2Cl_2 and washed twice with H_2O. The organic layer was dried over anhydrous Na_2SO_4 and evaporated to afford the crude product, which was isolated by flash column chromatography using petroleum ether/ethyl acetate (20 : 1,v/v) to give **CP5** 2.0219 g (38.66%) as a white solid. m.p.:185-189 ^oC. ^1H NMR (600 MHz, $CDCl_3$, room temperature) δ (ppm): 6.93(m, 10H),

3.82(m, 34H), 3.69(s, 4H), 1.49(m,16H), 0.87(m, 4H). ESI-MS m/z: [$C_{55}H_{68}O_{10}Br_2 + NH_4^+$] Calcd for 1066.3493; Found 1066.3496.

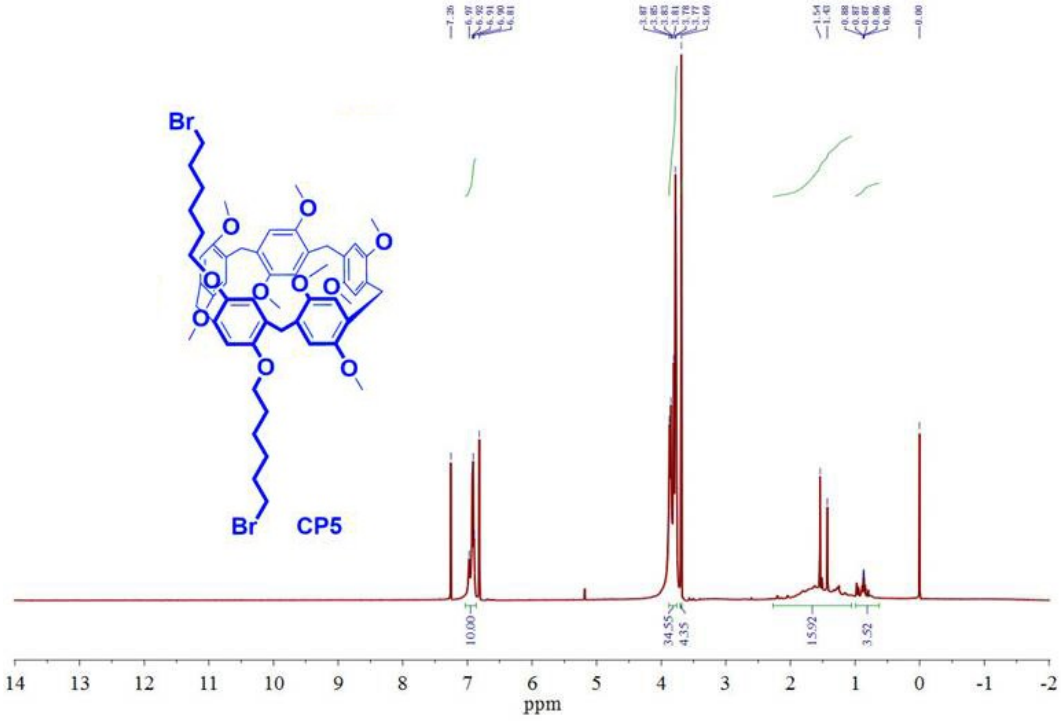

Fig. S13 ^{1}H NMR spectra (600 MHz, $CDCl_3$) of **CP5**.

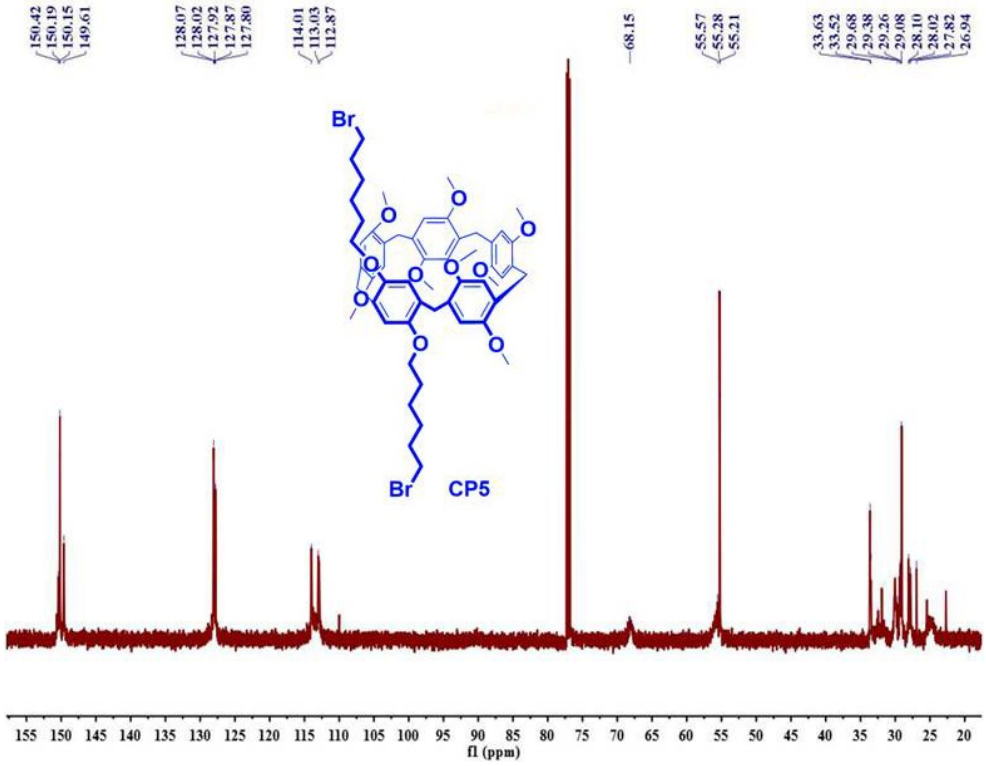

Fig. S14 ^{13}C NMR spectra (151 MHz, $CDCl_3$) of **CP5**.

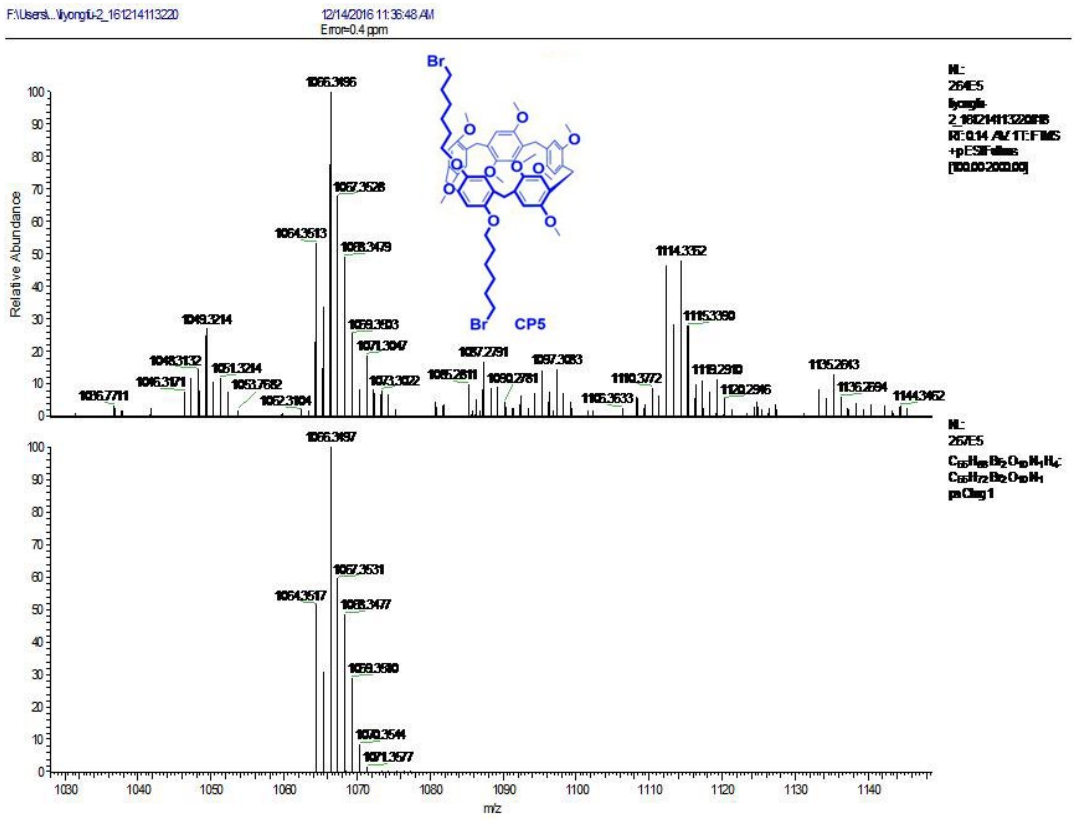

Fig. S15 High resolution mass data of compound **CP5**.

Synthesis of host compound WP5: Copillar[5]arene **CP5** (0.5 g, 0.5 mmol) and trimethylamine (33 % in ethanol, 1.0 mL, 3.7 mmol) were added to ethanol (80 mL). The solution was refluxed overnight. Then the solvent was removed by evaporation, you can afford a white solid. After white solid was washed by diethyl ether to obtain **WP5** as a white solid (0.52 g, 93 %). Mp 176−178 ^{o}C. ^{1}H NMR (400 MHz, DMSO-d_6) δ 7.00 – 6.67 (m, 10H), 3.95 (d, J = 70.8 Hz, 4H), 3.83 – 3.53 (m, 34H), 3.43 (t, J = 7.0 Hz, 4H), 3.07 (d, J = 6.1 Hz, 18H), 1.71 (s, 8H), 1.56 (s, 4H), 1.40 – 1.29 (m, 4H). ^{13}C NMR (151 MHz, DMSO-d_6) δ 150.34, 149.61, 128.04, 113.77, 68.08, 65.68, 55.99, 55.93, 55.91, 55.84, 52.61, 36.16, 31.18, 29.48, 26.17, 25.83, 22.54. ESI-MS m/z: [$C_{61}H_{86}$ $BrN_2O_{10}^{+}$] Calcd

for 1087.27; Found 1087.3384.

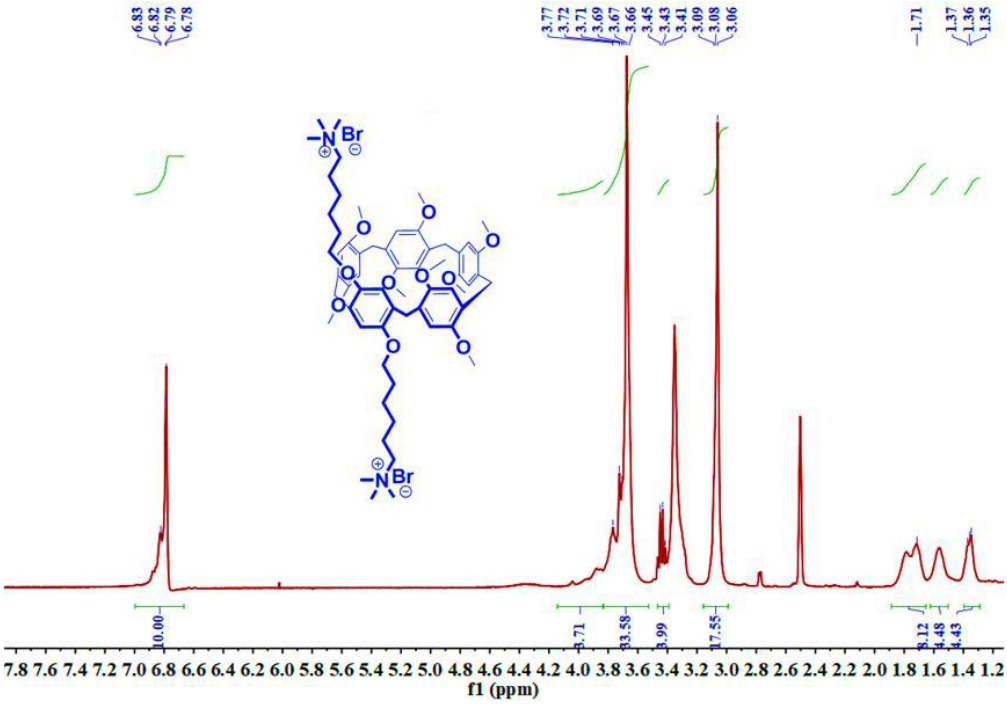

Fig. S16 ^{1}H NMR spectra (400 MHz, DMSO-d_6) of **WP5**.

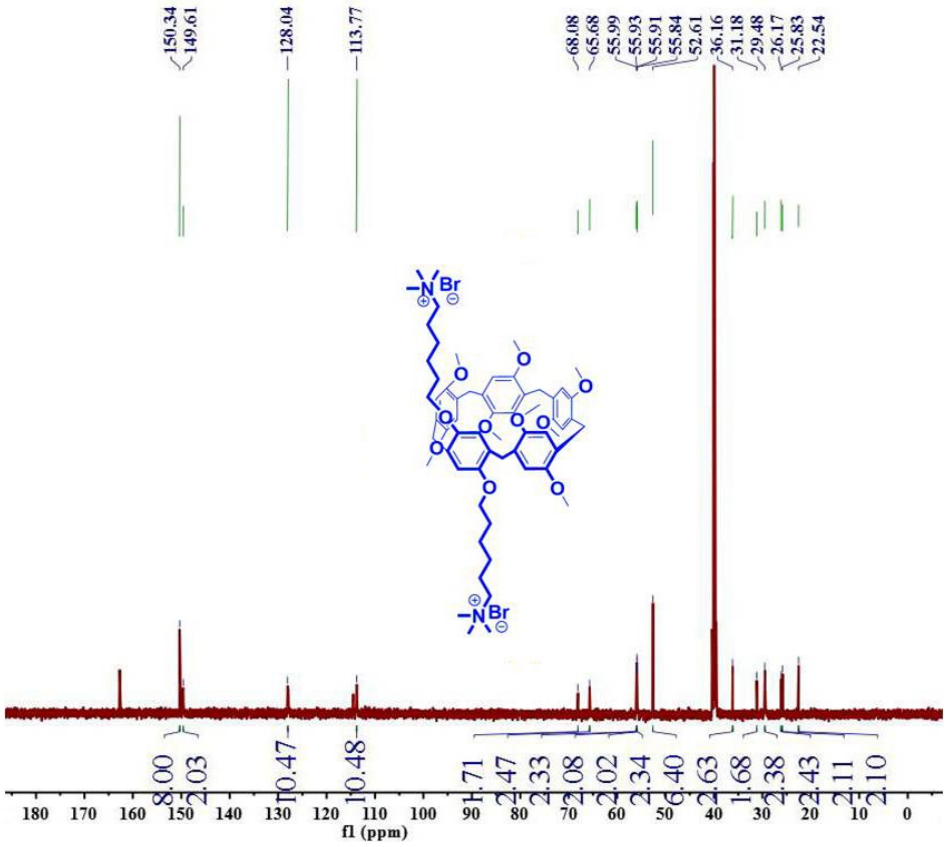

Fig. S17 ^{13}C NMR spectra (151 MHz, DMSO-d_6) of **WP5**.

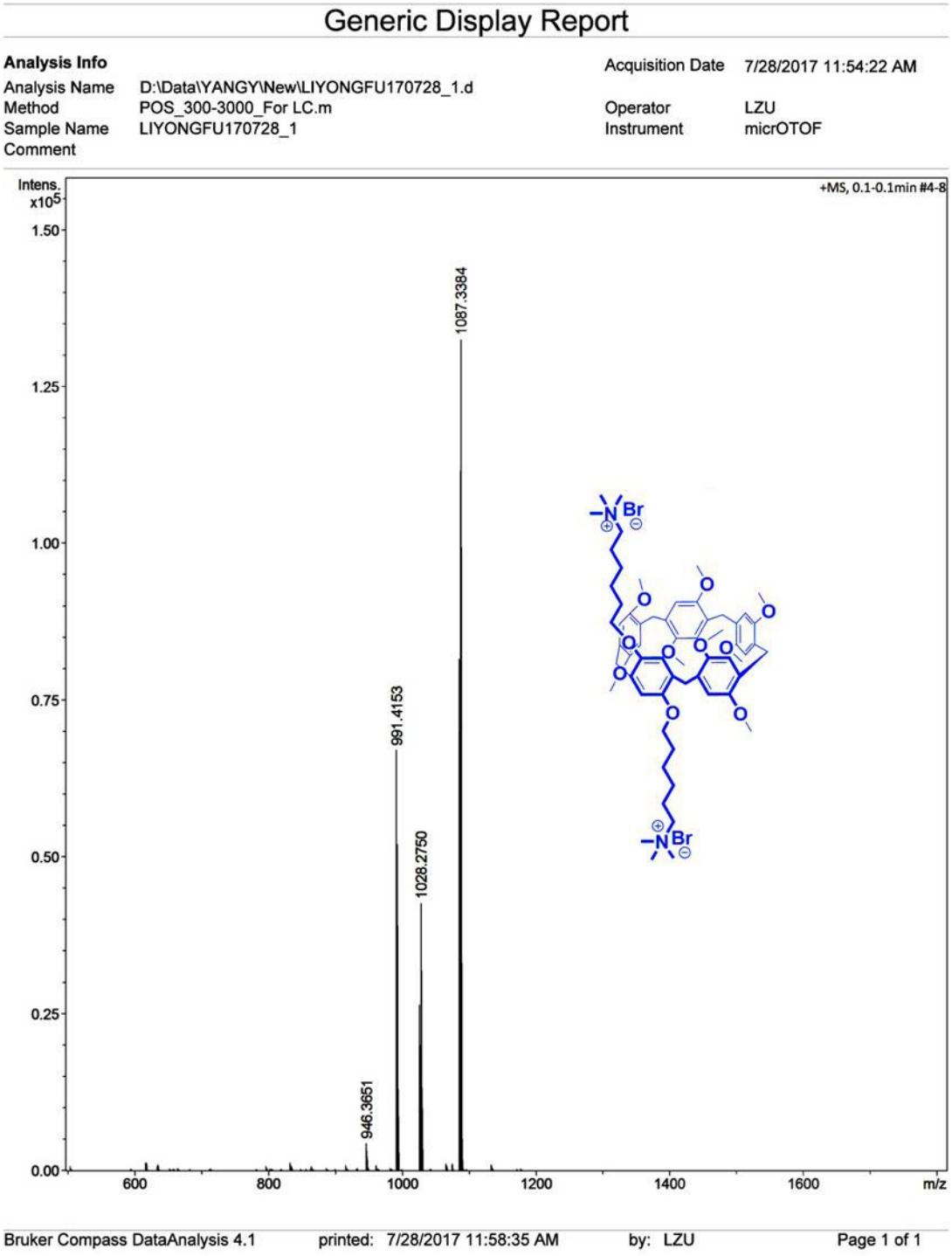

Fig. S18 ESI-MS spectrum of compound **WP5**.

Table S1. Gelation Property of supramolecular gel **WP5-PN-G**.

Entry	Solvent	State[a]	CGC[b](%)	Tgel[c] (^oC, wt%)
1	DMSO	S	\	\
2	DMSO/H_2O(1:1)	G	10.5%	52
3	DMF	S	\	\
4	DMF/H_2O(1:1)	P	\	\
5	CH_3CN	P	\	\
6	CH_3CN/H_2O	P	\	\
7	CH_3CH_2OH	P	\	\
8	CH_3CH_2OH/H_2O	P	\	\
9	CH_3OH	P	\	\
10	CH_2ClCH_2Cl	P	\	\
11	CH_2Cl_2	S	\	\
12	$CHCl_3$	S	\	\
13	THF	P	\	\
14	THF/H_2O	S	\	\
15	Acetone	P	\	\
16	ethyl acetate	P	\	\
17	isopentanol	P	\	\
18	n-hexane	P	\	\
19	cyclohexanol	G	14%	40
20	isopropanol	P	\	\
21	n-butyl alcohol	P	\	\
22	n-hexanol	P	\	\
23	n-propanol	P	\	\
24	tert butyl alcohol	P	\	\
25	petroleum ether	P	\	\
26	propionic acid	S	\	\
27	n-hexylic acid	S	\	\

State：n_{WP5}/n_{PN} =1/1

[a]G, P and S denote gelation, precipitation and solution, respectively.

[b]The critical gelation concentration (wt%, 10mg/ml = 1.0%).

[c]The gelation temperature (^oC).

Table S2. Optimum water content of gelation conditions

Entry	Water content	State[a]	Tgel[b] (°C)
1	0%	S	\
2	5%	S	\
3	10%	P	\
4	20%	P	\
5	30%	P	\
6	40%	P	\
7	50%	G	52
8	60%	G	46
9	70%	P	\
10	80%	P	\

[a]G, P and S denote gelation, precipitation and solution, respectively.

[b]The critical gelation concentration (wt%, 10mg/ml = 1.0%).

[c]The gelation temperature (°C). C = 90 mM.

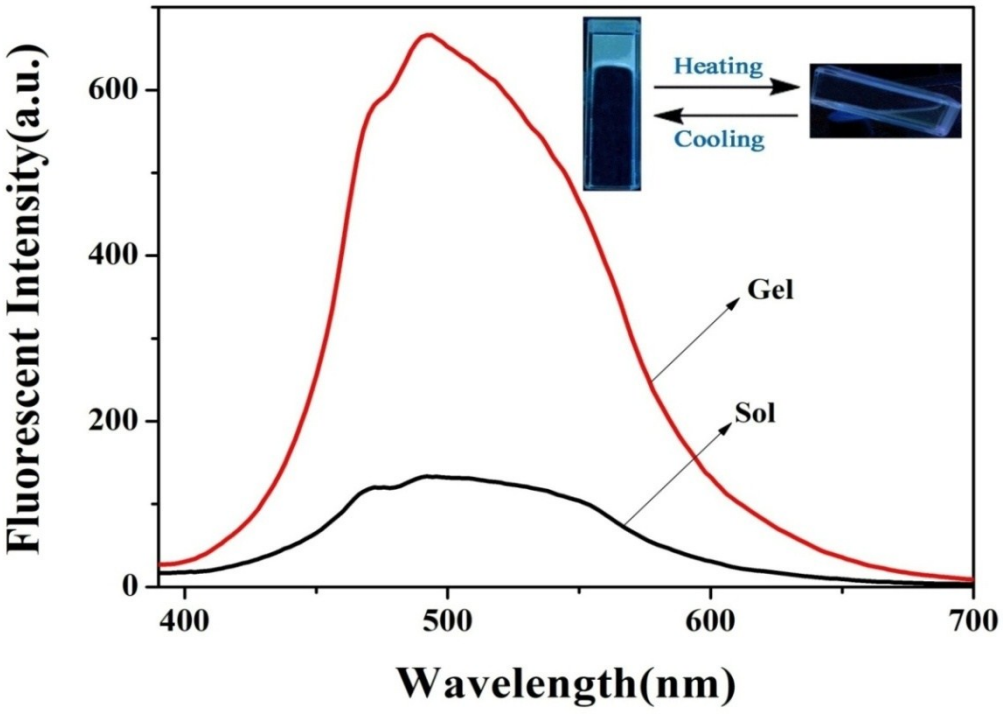

Fig. S19 Fluorescence spectra of supramolecular gel **WP5-PN-G** (in gelated state, 10.5 %, w/v) and solution in the DMSO-H_2O (1:1, v/v) system (λ_{ex} =365 nm).

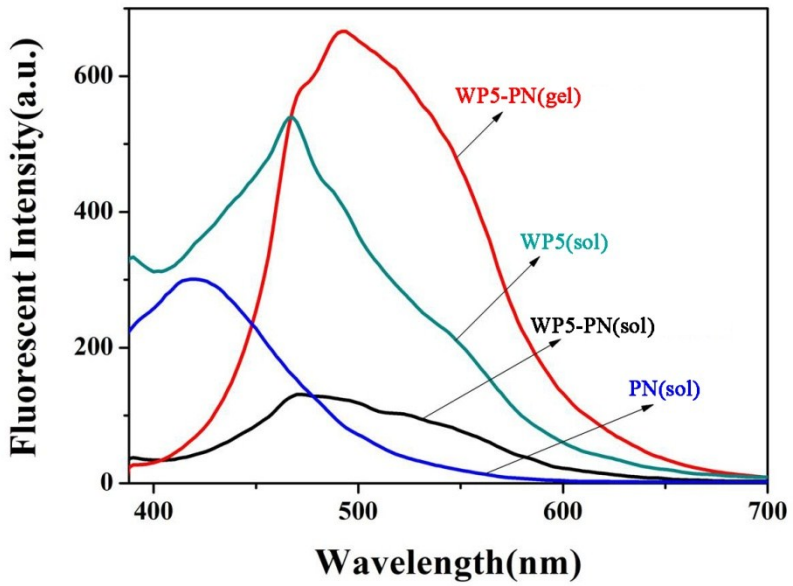

Fig. S20 Fluorescence spectra of **WP5** (c = 90 mM), **PN** (c = 87 mM), **WP5-PN** sol (c = 90 mM, T = 85 °C > T_{gel}) and the **WP5-PN-G** (in the DMSO-H_2O (1:1, v/v) system, c = 90 mM, T = 20 °C < T_{gel}, λ_{ex} =365 nm).

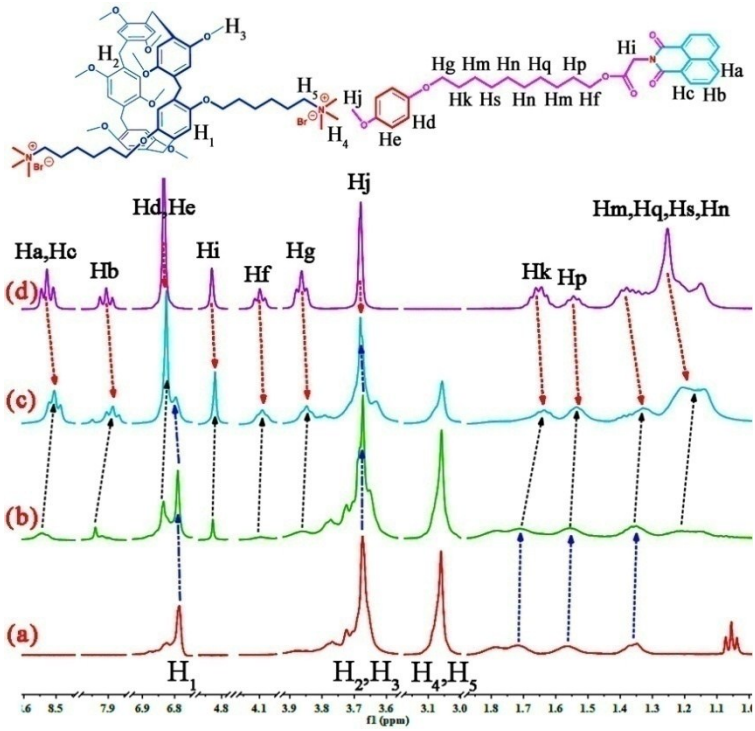

Fig. S21 Partial ^{1}H NMR spectra of **WP5** (0.017 mol/L) in DMSO-d_6 with increasing amounts of **PN**, (a) Free **WP5**; (b) 0.5 equiv. (c) 2.0 equiv. (d) Free **PN**.

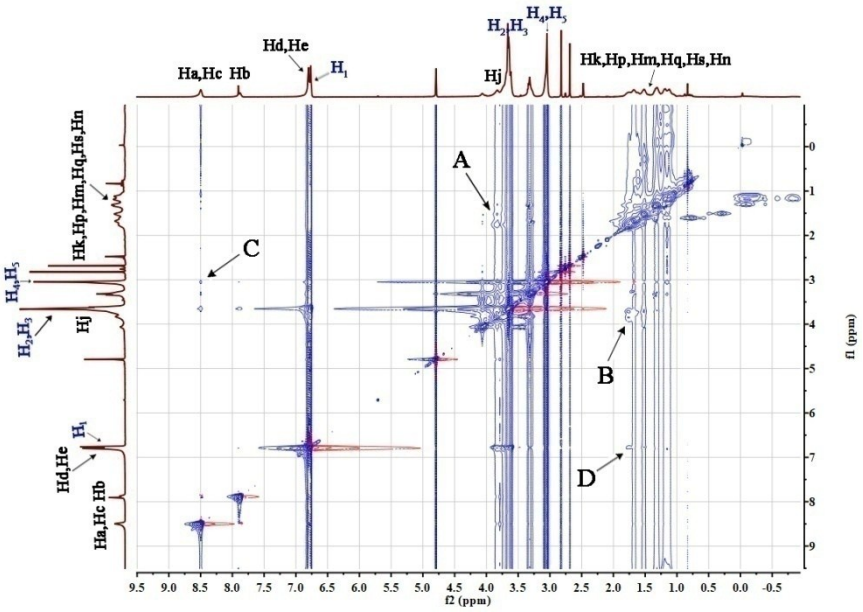

Fig. S22 2D NOESY NMR spectrum (600 MHz, 298 K) of 50.0 mM **WP5** and **PN** in DMSO-d_6 solution.

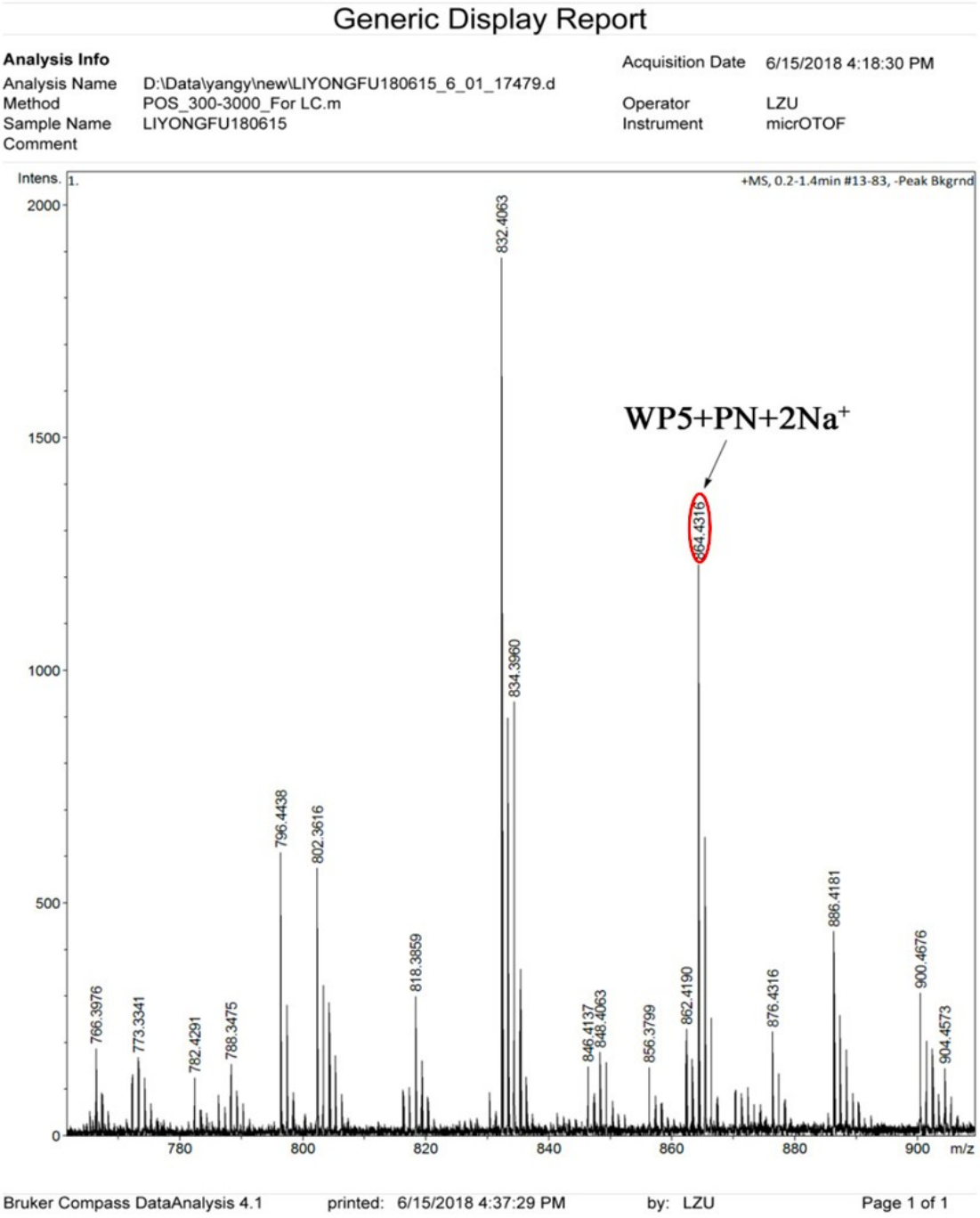

Fig. S23 ESI-MS spectrum of the host-guest complex formed between **WP5** and **PN**.

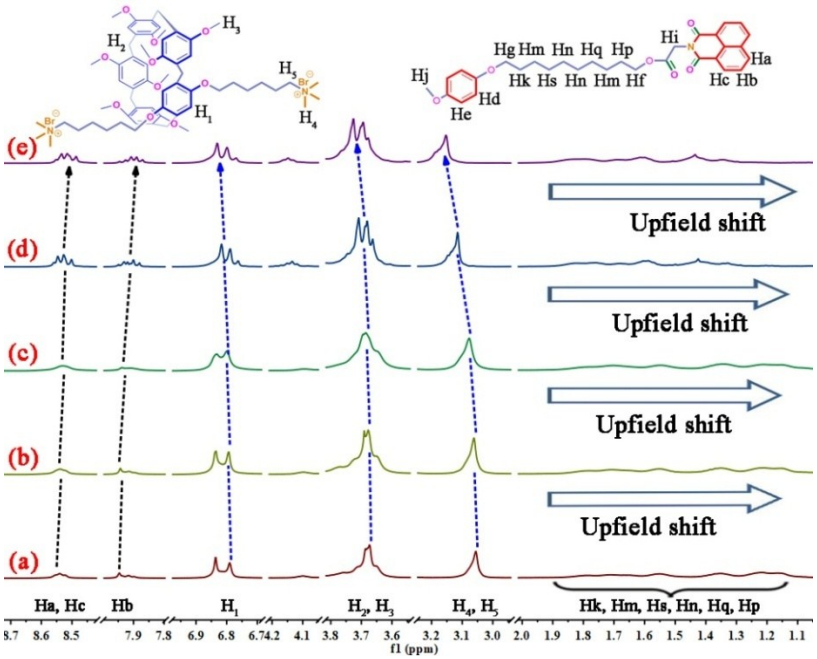

Fig. S24 ^{1}H NMR spectra (600 MHz, 298 K) of **WP5-PN** in DMSO-d_6 at various concentrations: (a) 1.0 mM; (b) 2.0 mM; (c) 5.0 mM; (d) 10.0 mM; (e) 20.0 mM.

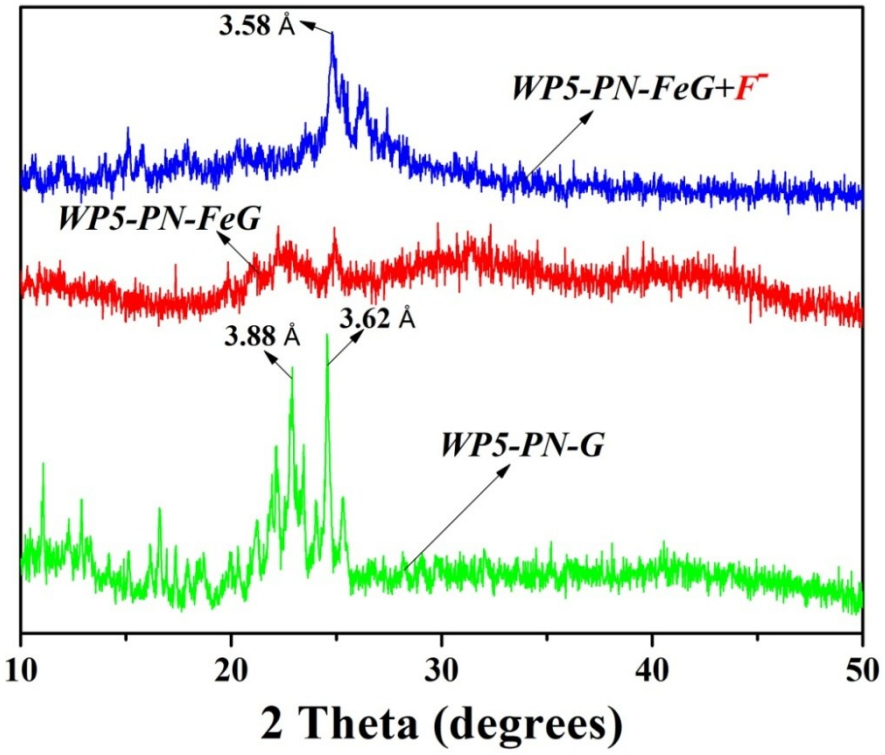

Fig. S25 XRD diagrams of xerogel of **WP5-PN-G**, metallogel of **WP5-PN-FeG**, xerogel of **WP5-PN-FeG** +F^-.

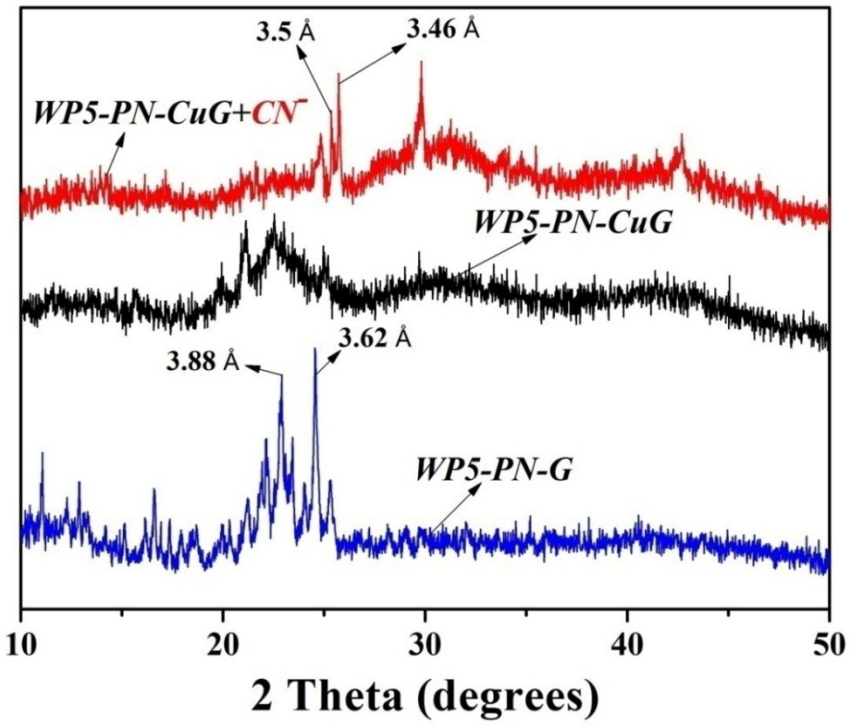

Fig. S26 XRD diagrams of xerogel of **WP5-PN-G**, metallogel of **WP5-PN-CuG** and xerogel of **WP5-PN-CuG** +CN^-.

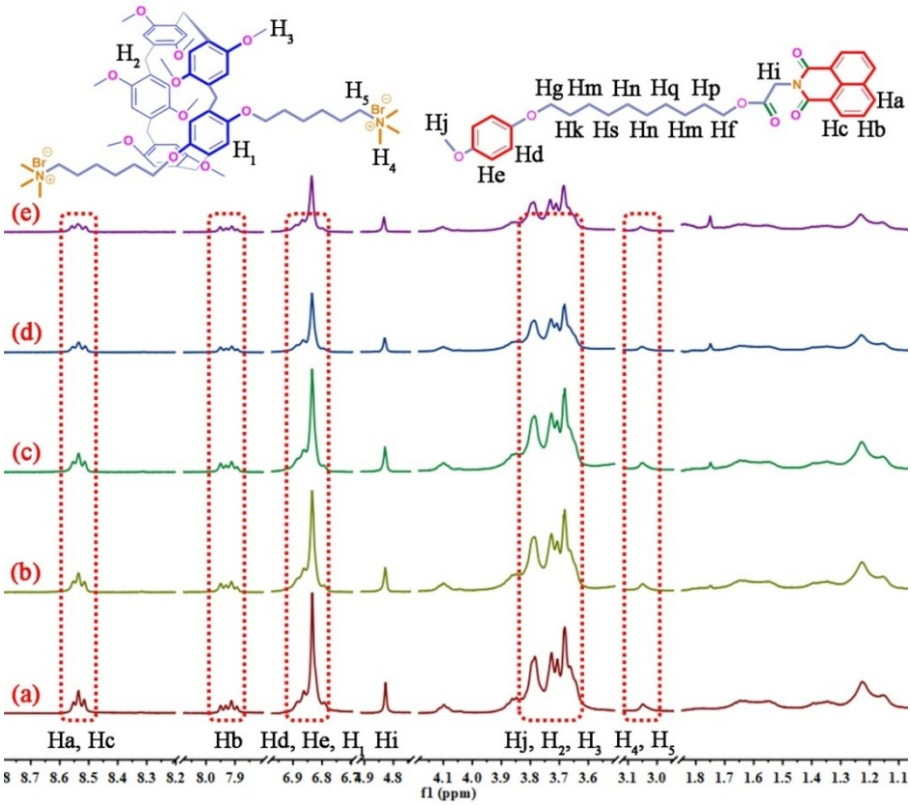

Fig. S27 Partial ^{1}H NMR spectra (600 MHz, DMSO-d_6, 298 K) of **WP5-**

PN and CH_3COOH at various concentrations: (a) 5.0 mM; (b) 8.0 mM; (c) 10.0 mM; (d) 15.0 mM; (e) 20.0 mM.

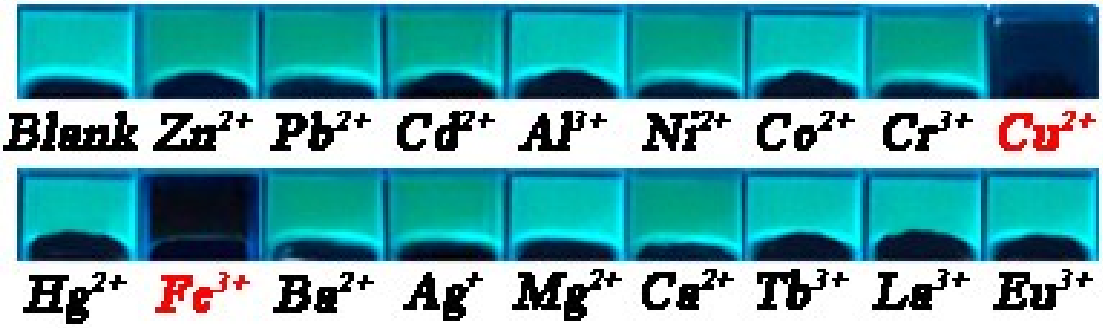

Fig. **S28** Photographs of organogel of **WP5-PN-G** (10.5% w/v) in DMSO-H_2O (1:1, v/v) system and organogels of **WP5-PN-G** in the presence of various metal ions (Zn^{2+}, Pb^{2+}, Cd^{2+}, Al^{3+}, Cr^{3+}, Ni^{2+}, Co^{2+}, Cu^{2+}, Hg^{2+}, Fe^{3+}, Ba^{2+}, Ag^{+}, Mg^{2+}, Ca^{2+}, Tb^{3+}, La^{3+} and Eu^{3+}) under UV light.

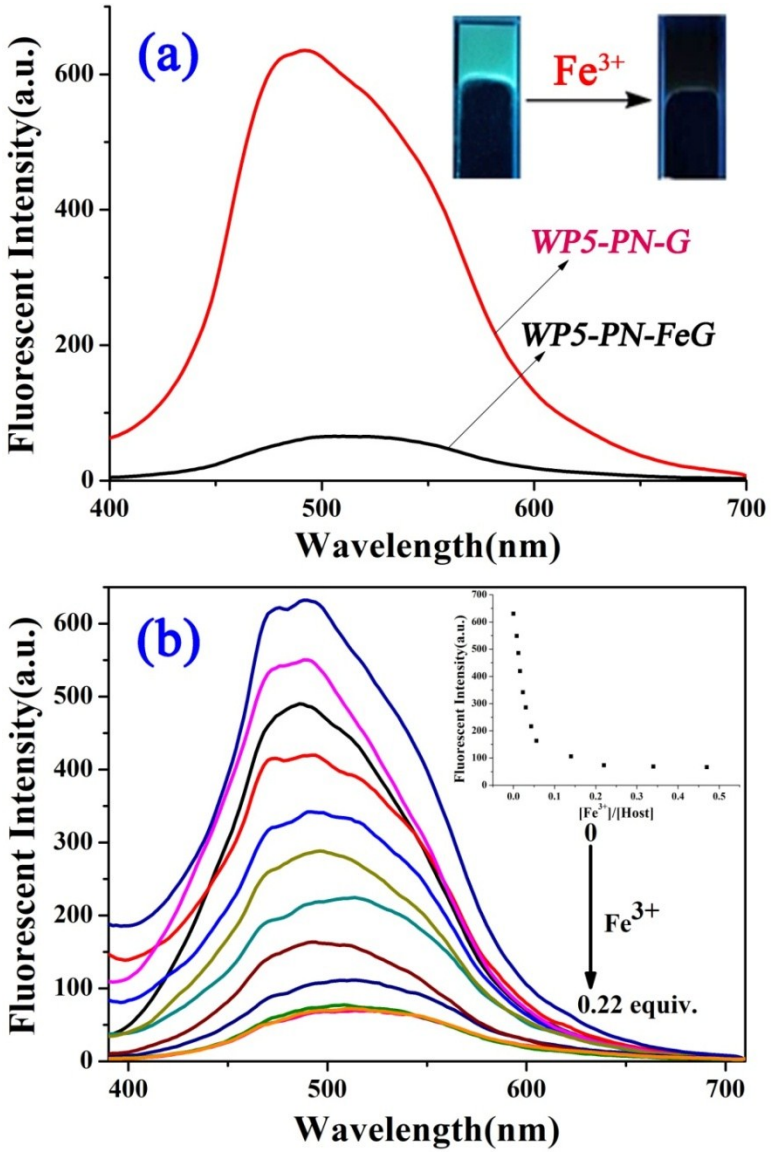

Fig. S29 Fluorescence spectra of supramolecular gel (a) **WP5-PN-G** and **WP5-PN-FeG** (10.5%, in DMSO-H_2O (v:v = 1:1) binary solution, **WP5-PN** = 1:1). (b) The fluorescence spectra of **WP5-PN-G** (10.5%, in DMSO-H_2O (v:v=1:1) binary solution, **WP5-PN** = 1:1) with increasing concentration of Fe^{3+} (using 0.1 mol L^{-1} Fe^{3+} water solution as the Fe^{3+} sources), λ_{ex} = 365 nm.

Determination of the detection limit

We use the 3δ way to figure out the detection limit. The process of the analysis as follows.

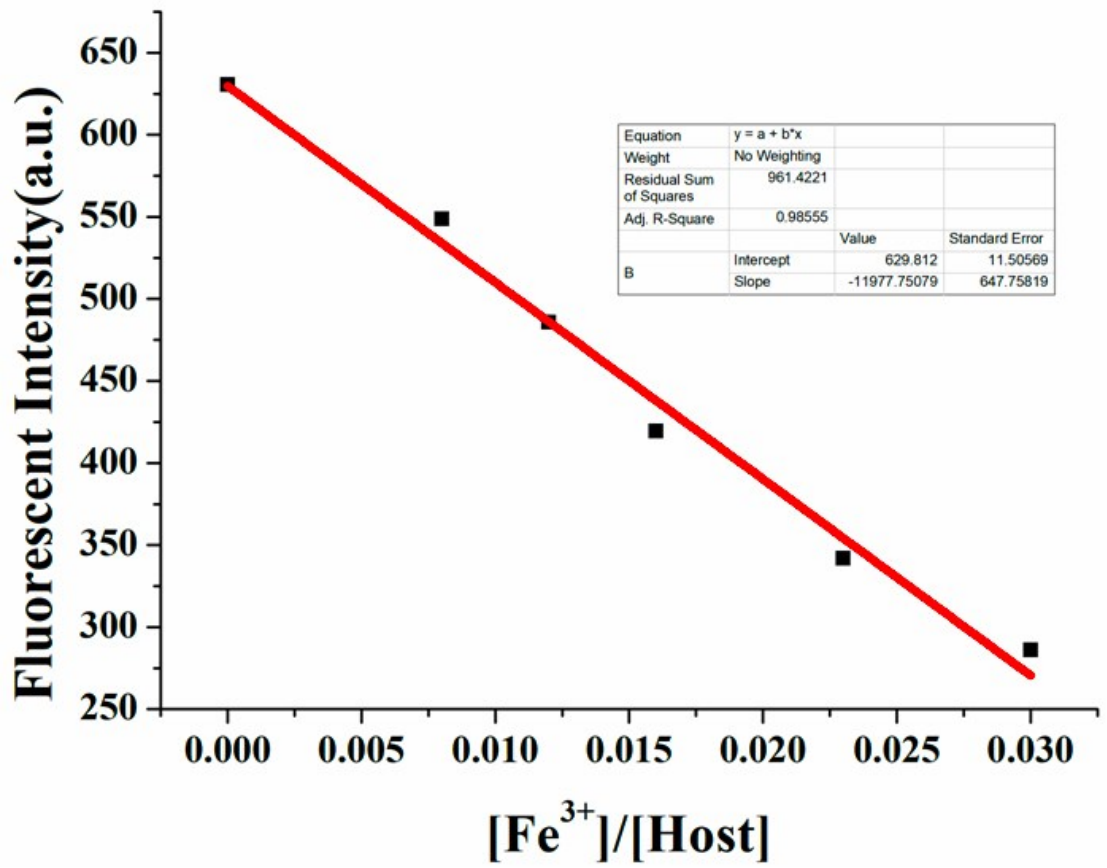

Fig. S30 Plot of the intensity at 492 nm for a mixture of **WP5-PN-G** and Fe^{3+} (λ_{ex}= 365 nm).

Linear Equation: Y=−11977.75079X+629.812 R^2=0.98555

S=11977.75×10^6

$$\delta = \sqrt{\frac{\sum(Fi-F0)^2}{N-1}} = 2.505324(N=20)$$

K=3

LOD =K×δ/S=6.27×10^{-10} M

Fi is the fluorescence intensity of **WP5-PN-G**; F0 is the average of the Fi.

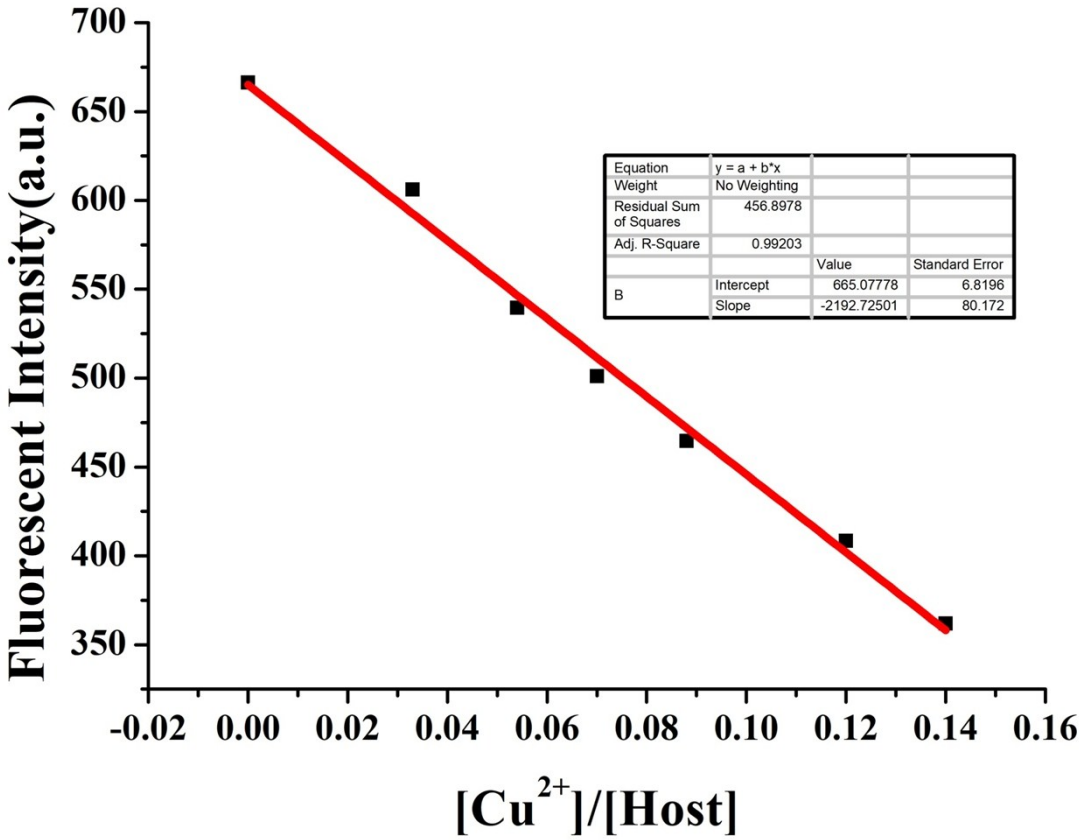

Fig. S31 Plot of the intensity at 492 nm for a mixture of **WP5-PN-G** and Cu^{2+} in DMSO-H_2O (1:1, v/v) solution (λ_{ex} = 365 nm).

Linear Equation: Y=−2192.72501X+665.07778 R^2=0.99203

S=2192.73×10^6

$$\delta = \sqrt{\frac{\sum(Fi-F0)^2}{N-1}}$$ = 3.326178 (N=20)

K=3

LOD =K×δ/S= 4.55×10^{-9} M

Fi is the fluorescence intensity of **WP5-PN-G**; F0 is the average of the Fi.

Table S3. A part of the literatures about the LOD (mol/L) of cations and anions (Fe^{3+}, Cu^{2+}, F^- and CN^-) were provided in the followed table.

Ref.	for Fe^{3+}	for Cu^{2+}	for F^-	for CN^-
[S1]	5.15×10^{-7} M	-	-	-
[S2]	-	1.21×10^{-6} M	-	-
[S3]	-	-	8×10^{-7} M	-
[S4]	-	-	1.3×10^{-6} M	7.98×10^{-7} M
[S5]	1×10^{-8} M	-	-	-
[S6]	-	2.0×10^{-7} M	-	-
[S7]	-	-	1.2×10^{-7} M	-
[S8]	-	-	-	4×10^{-7} M
[S9]	2.5×10^{-8} M	-	-	-
[S10]	-	1.0×10^{-6} M	-	-
[S11]	-	-	5.9×10^{-7} M	-
[S12]	-	2.28×10^{-7} M	-	1.33×10^{-8} M
[S13]	2×10^{-8} M	-	-	-
[S14]	-	5.0×10^{-8} M	-	-
[S15]	-	-	2.6×10^{-7} M	
[S16]	-	-	-	5.92×10^{-7} M
[S17]	1.0×10^{-7} M	-	-	-
[S18]	-	1.0×10^{-7} M	-	-
[S19]	-	-	2.0×10^{-6} M	-
[S20]	-	7×10^{-8} M	-	-
[S21]	2.05×10^{-8} M	-	-	-
This work	6.27×10^{-10}	4.55×10^{-9}	1.0×10^{-8}	1.0×10^{-8}

Table S4 Adsorption percentage of **WP5-PN-G** for Fe^{3+} and Cu^{2+}.

Ions	Initial concentration (M)	Residual concentration(M)	Adsorption percentage %
Fe^{3+}	1×10^{-4}	1.93×10^{-6}	98.07
Cu^{2+}	1×10^{-4}	4.62×10^{-6}	95.38

Calculation method of adsorption percentage:

$$\text{Adsorption percentage}(\%) = \left(1 - \frac{C_R \times V_R}{C_I \times V_I}\right) \times 100\%$$

(state: C_R is the residual concentration of Fe^{3+}, C_I is the initial concentration of Fe^{3+}, V_R=V_I)

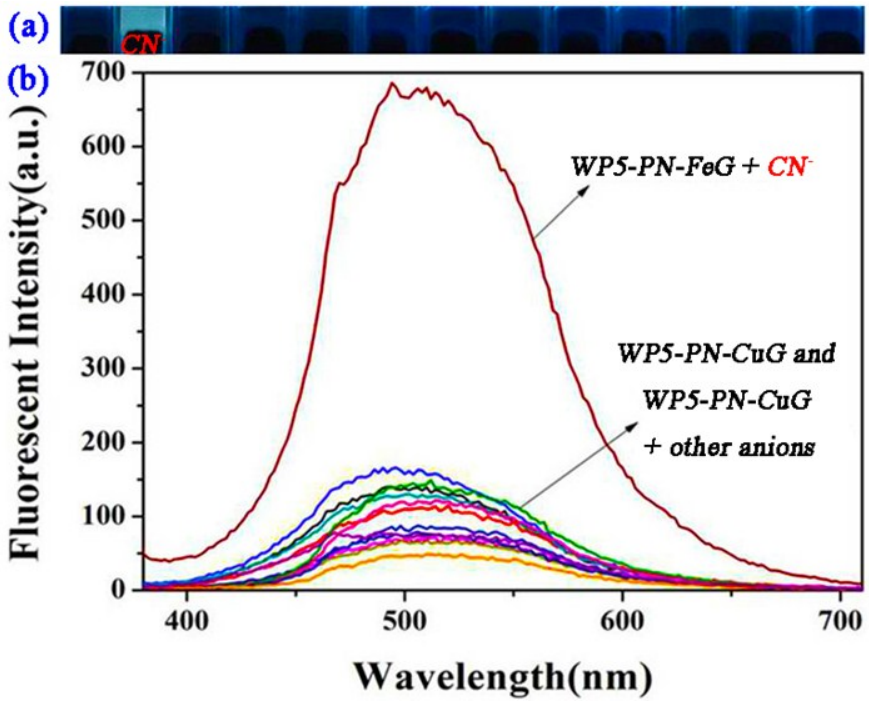

Fig. S32 (a) Photographs of **WP5–PN-CuG** in the DMSO-H_2O (1:1, v/v) system (10.5 %, w/v) and **WP5–PN-CuG** in the presence of various anions under UV light. (b) Fluorescence spectra of **WP5–PN-CuG** and **WP5–PN-CuG** (in gelated state) in the presence of various anions, (λ_{ex} =365 nm).

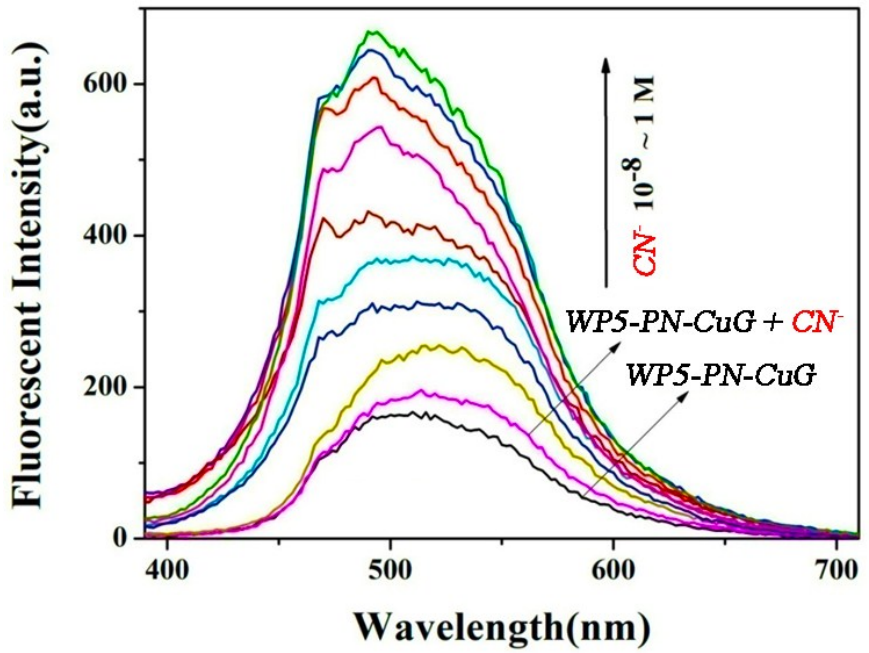

Fig. S33 Fluorescence spectra of supramolecular metallogel **WP5-PN-**

CuG (10.5%, w/v) with increasing concentration of CN^- (using 1.0 M NaCN water solution as the CN^- source), λ_{ex} = 365 nm.

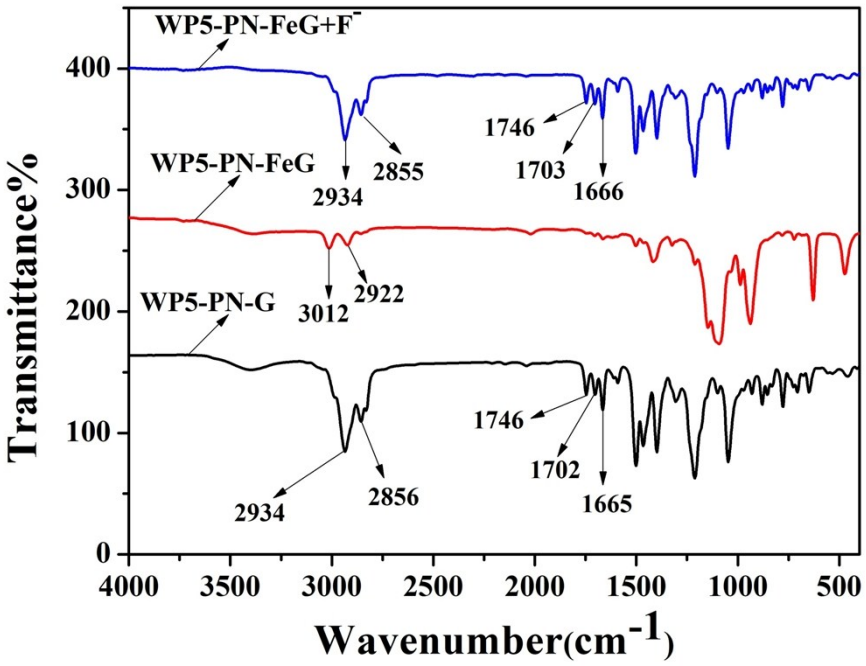

Fig. **S34** FT-IR spectra of xerogel of **WP5-PN-G**, metallogel **WP5-PN-FeG** and **WP5-PN-FeG** +F^-.

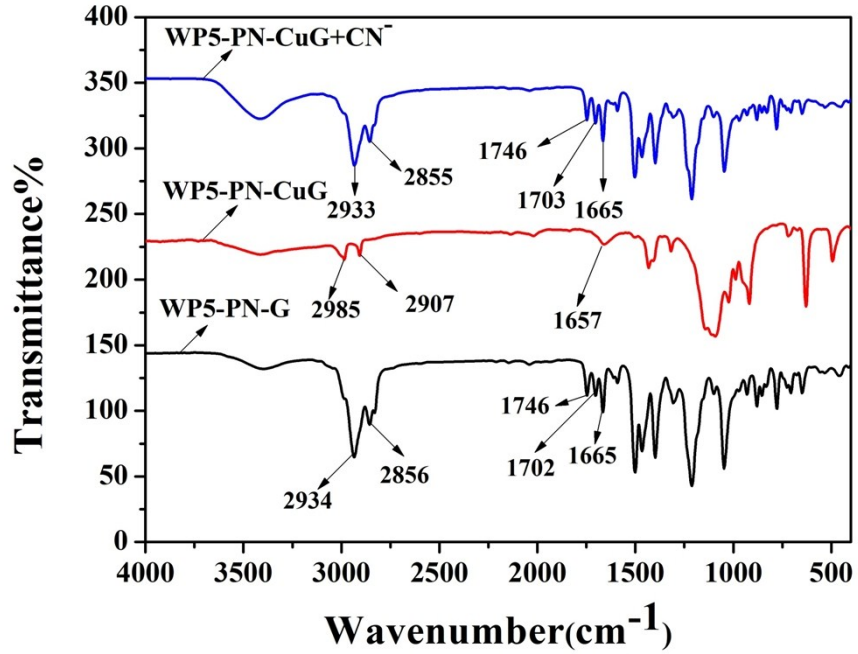

Fig. S35 FT-IR spectra of xerogel of **WP5-PN-G**, metallogel **WP5-PN-CuG** and **WP5-PN-CuG** +CN^-.

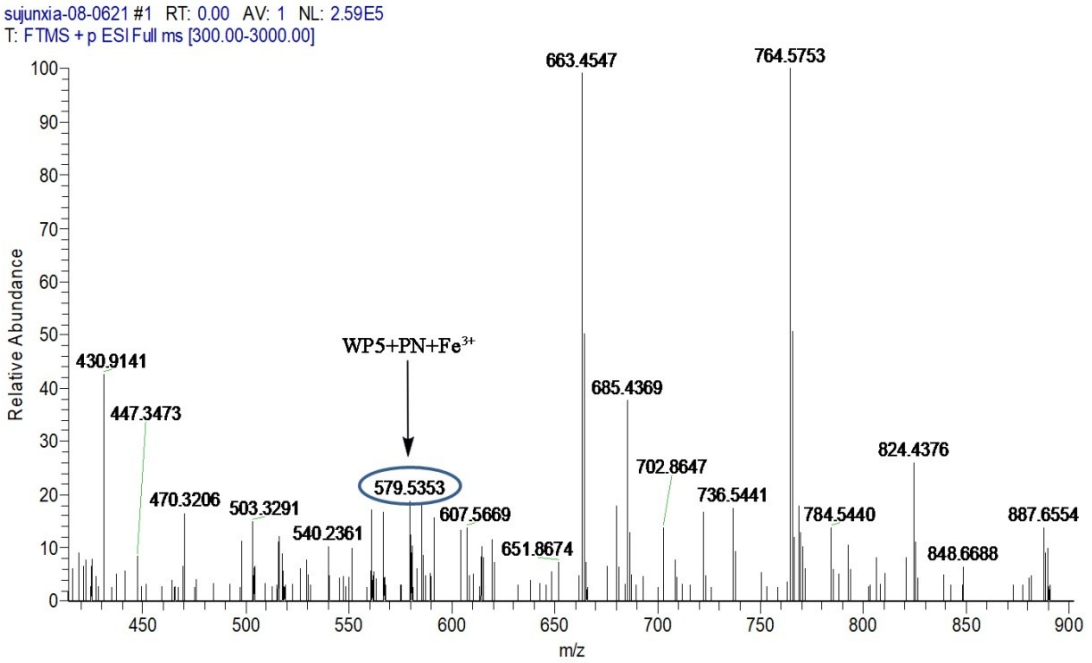

Fig. S36 ESI-MS spectrum of **WP5-PN**-Fe^{3+}.

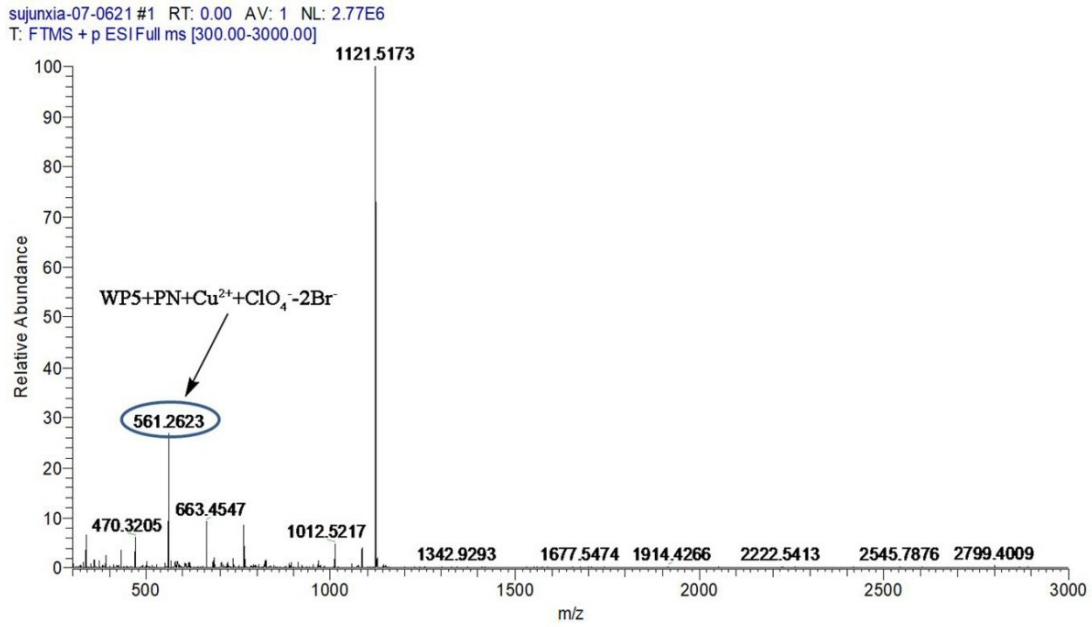

Fig. S37 ESI-MS spectrum of **WP5-PN**-Cu^{2+}.

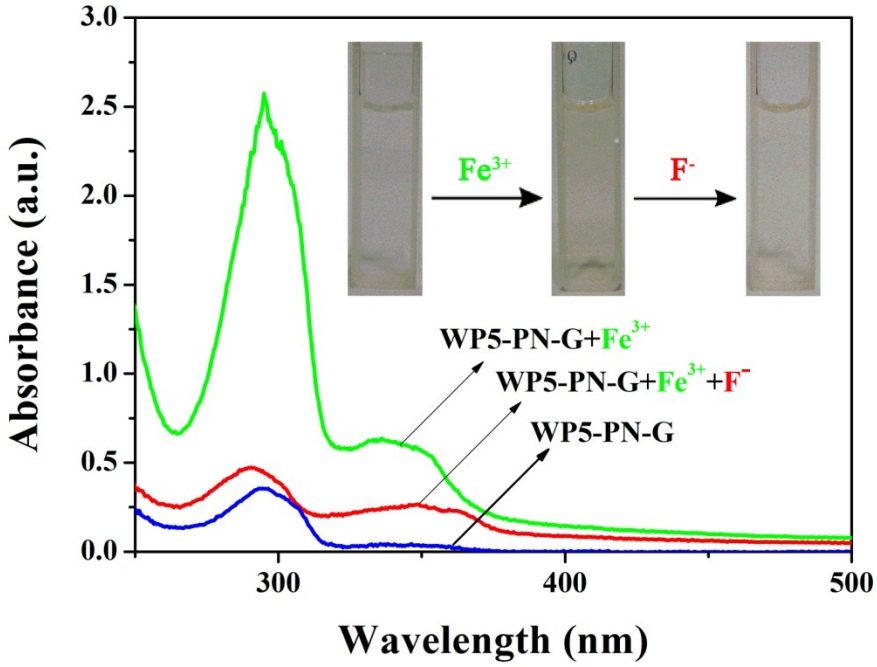

Fig. S38 Absorbance spectra of **WP5-PN-G** (2.0×10^{-5} M) in DMSO-H_2O (1:1, v/v) solution upon the addition of Fe^{3+} (5.0 equiv.) and F^- (20.0 equiv.). Inset: photograph showing the change in color of the solution of **WP5-PN-G** in DMSO-H_2O (1:1, v/v) solution after addition of Fe^{3+} and F^- at room temperature.

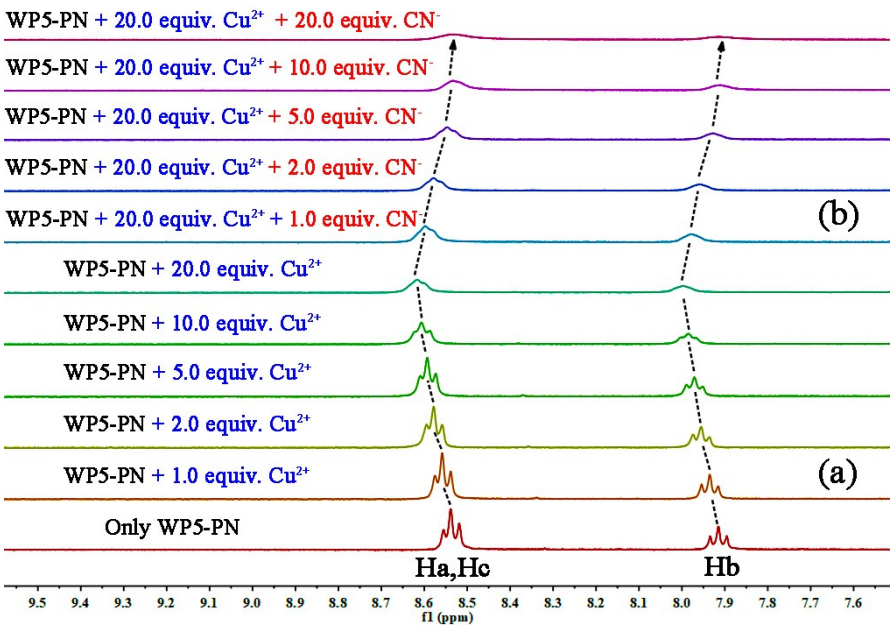

Fig. S39 Partial ^{1}H NMR spectra (600 MHz, DMSO-d_6, 298 K) of (a) **WP5-PN** in the presence of varying amounts of Cu^{2+} and (b) **WP5-PN** + Cu^{2+} in the presence of varying amounts of CN^{-}.

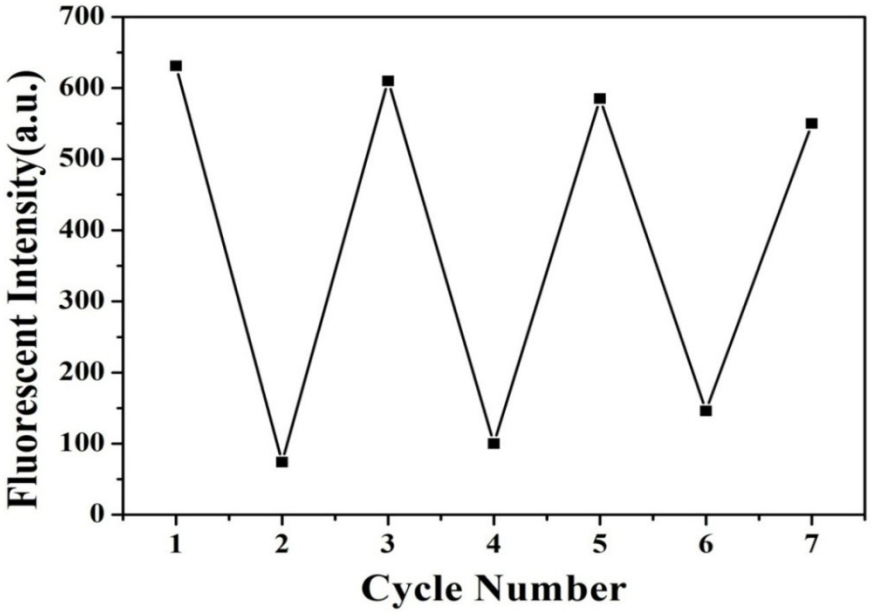

Fig. S40 Emission spectra showing the reversible evidence between **WP5-PN-G** and Fe^{3+} by introduction of F^{-} (λ_{ex} = 365 nm).

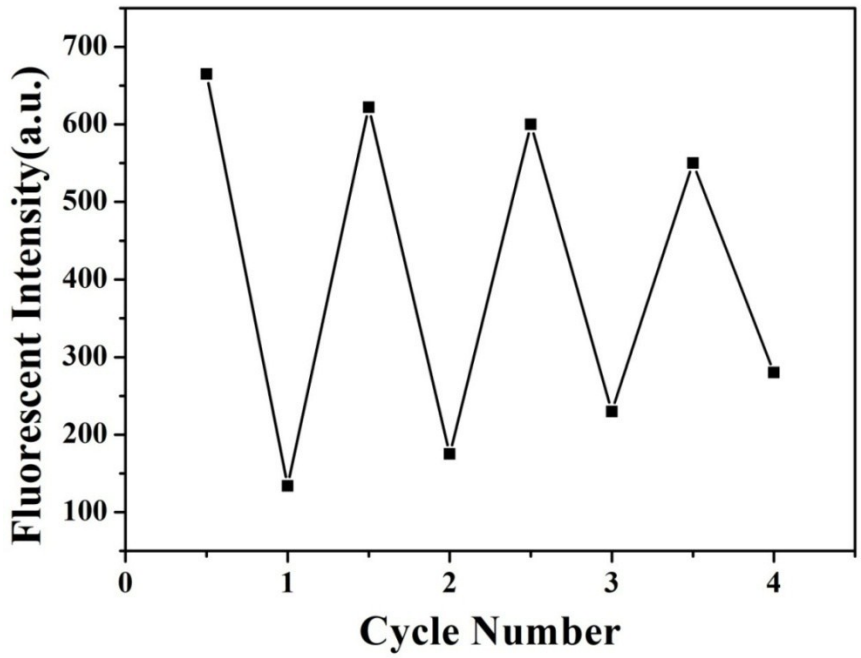

Fig. S41 Fluorescent ‘‘Off–On–Off’’ cycles of **WP5-PN-G** controlled by the alternating addition of Cu^{2+} and CN^{-}, (λ_{ex} = 365 nm).

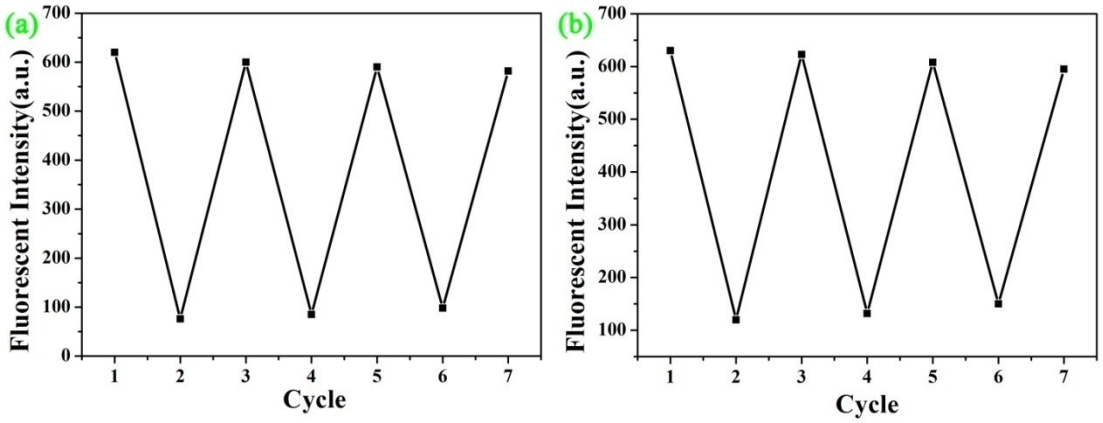

Fig. S42 (a) Recyclable separation of Fe^{3+} (λ_{ex} = 365 nm), (b) Recyclable separation of Cu^{2+} (λ_{ex} = 365 nm).

References:

[S1] B.-X. Shen and Y. Qian, *J. Mater. Chem. B*., 2016, **4**, 7549-7559.

[S2] H. Shao, Y. D. Ding, X. Hong and Y. C. Liu, *Analyst*, 2018, **143**, 409-414 .

[S3] J. Hu, C. Li, Y. Cui and S. Liu, *Macromol. Rapid Commun*., 2011, **32**, 610.

[S4] R. Ali, R. C. Gupta, S. K. Dwivedi and A. Misra, *New J. Chem.*, 2018, **42**, 11746-11754.

[S5] C. X. Wang, Y. J. Huang, K. L. Jiang, M. G. Humphrey and C. Zhang, *Analyst*, 2016, **141**, 4488-4494.

[S6] B. N. Ahamed and P. Ghosh, *Dalton Trans.,* 2011, **40**, 6411–6419.

[S7] X.Cao, W. Lin, Q. Yu and J. Wang, *Org. Lett*., 2011, **13**, 6098.

[S8] *Y. Shiraishi, M. Nakamura, K. Yamamoto and T. Hirai, Chem. Commun*., 2014, **50**, 11583-11586.

[S9] T. Zhou , X. X. Chen, Q. H. Hua, W. Lei, Q. L. Hao, B. J. Zhou, C. Su and X. F. Bao, *Sensors and Actuators B*., 2017, **253**, 292–301.

[S10] H. Seo, M. An, B. Y. Kim, J. H. Choi, A. Helal and H. S. Kim, *Tetrahedron*, 2017, **73**, 4684–4691.

[S11] J. Ren, Z. Wu, Y. Zhou, Y. Li and Z. Xu, *Dyes Pigm*., 2011, **91**, 442.

[S12] L. Y. Qin, L. J. Hou, J. Feng, J. B. Chao, Y. Wang and W. J. Jin, *Anal. Methods*., 2017, **9**, 259-266.

[S13] R. H. Guo, S. X. Zhou, Y. C. Li, X. H. Li, L. Z. Fan and N. H. Voelcker, *ACS Appl. Mater. Interfaces*, 2015, **7**, 23958–23966.

[S14] Y. Li, H. Zhou, S. Yina, H. Jiang, N. Niu, H. Huang, S. A. Shahzad and C. Yu, *Sens. Actuators, B*, 2016, **235**, 33–38.

[S15] M. Kumar, R. Kumar and V. Bhalla, *Tetrahedron*., 2009, **65**, 4340.

[S16] C. S. Liang and S. M. Jiang, *Analyst.*, 2017, **142**, 4825-4833.

[S17] J. Wang, M. Jiang, L. Yan, R. Peng, M. J. Huangfu, X. X. Guo, Y. Li and P.Y. Wu, *Inorg. Chem.*, 2016, **55**, 12660–12668.

[S18] L. Huang, J. Cheng, K. Xie, P. Xi, F. Hou, Z. Li, G. Xie, Y. Shi, H. Liu, D. Bai and Z. Zeng, *Dalton Trans.,* 2011, **40**, 10815–10817.

[S19] W. Huang, H. Lin, Z. Cai and H. Lin, *Talanta.,* 2010, **81**, 967.

[S20] L. Chen, Z. P. Song, X. T. Liu, L. Q. Guo, M.-J. Li and F. F. Fu, *Analyst*, 2018, **143**, 1609-1614.

[S21] H. L. Wu, L. Yang, L. F. Chen, F. Xiang and H. Y. Gao, *Anal.*

Methods, 2017, **9**, 5935-5942.